

PAPER • OPEN ACCESS

# Pivotal issues on relativistic electrons in ITER

To cite this article: Allen H. Boozer 2018 *Nucl. Fusion* **58** 036006

View the [article online](#) for updates and enhancements.

## You may also like

- [Magnetic surface loss and electron runaway](#)  
Allen H Boozer
- [Wave train selection by invasion fronts in the FitzHugh–Nagumo equation](#)  
Paul Carter and Arnd Scheel
- [Synthesis of the European ALARA network 18th workshop 'ALARA for decommissioning and site remediation'](#)  
Sylvain Andresz, Julie Gilchrist, Ignacio Calavia Gimenez et al.

# Pivotal issues on relativistic electrons in ITER

Allen H. Boozer

Columbia University, New York, NY 10027, United States of America

E-mail: [ahb17@columbia.edu](mailto:ahb17@columbia.edu)

Received 28 November 2016, revised 29 November 2017

Accepted for publication 14 December 2017

Published 15 January 2018



## Abstract

The transfer of the plasma current from thermal to relativistic electrons is a threat to ITER achieving its mission. This danger is significantly greater in the nuclear than in the non-nuclear phase of ITER operations. Two issues are pivotal. The first is the extent and duration of magnetic surface breaking in conjunction with the thermal quenches. The second is the exponential sensitivity of the current transfer to three quantities: (1) the poloidal flux change required to e-fold the number of relativistic electrons, (2) the time  $\tau_a$  after the beginning of the thermal quench before the accelerating electric field exceeds the Connor-Hastie field for runaway, and (3) the duration of the period  $\tau_{op}$  in which magnetic surfaces remain open. Adequate knowledge does not exist to devise a reliable strategy for the protection of ITER. Uncertainties are sufficiently large that a transfer of neither a negligible nor the full plasma current to relativistic electrons can be ruled out during the non-nuclear phase of ITER. Tritium decay can provide a sufficiently strong seed for a dangerous relativistic-electron current even if  $\tau_a$  and  $\tau_{op}$  are sufficiently long to avoid relativistic electrons during non-nuclear operations. The breakup of magnetic surfaces that is associated with thermal quenches occurs on a time scale associated with fast magnetic reconnection, which means reconnection at an Alfvénic rather than a resistive rate. Alfvénic reconnection is well beyond the capabilities of existing computational tools for tokamaks, but its effects can be studied using its property of conserving magnetic helicity. Although the dangers to ITER from relativistic electrons have been known for twenty years, the critical issues have not been defined with sufficient precision to formulate an effective research program. Studies are particularly needed on plasma behavior in existing tokamaks during thermal quenches, behavior which could be clarified using methods developed here.

Keywords: runaway electrons, thermal quench, current spike, tokamak disruptions

(Some figures may appear in colour only in the online journal)

## 1. Introduction

The construction of ITER has placed scientific challenges on the plasma physics community. Perhaps none is greater than that of the transfer of the plasma current from thermal to relativistic electrons, which could result in unacceptable damage to the device.



Original content from this work may be used under the terms of the [Creative Commons Attribution 3.0 licence](https://creativecommons.org/licenses/by/3.0/). Any further distribution of this work must maintain attribution to the author(s) and the title of the work, journal citation and DOI.

To achieve its mission, less than one in a thousand ITER pulses can result in the transfer of a significant fraction of the plasma current to relativistic electrons that subsequently strike the walls [1]. Consequently, (1) ITER operations must be constrained to avoid rapid quenches in the electron temperature, (2) either natural or mitigation techniques must prevent electrons from running away to relativistic energies, or (3) relativistic electron currents must be benignly terminated.

The reliable termination of a plasma current faster than its natural decay without disruption, especially at a safety factor less than ten, has not been demonstrated and may be

impossible. This complicates the termination of relativistic currents and the avoidance of thermal quenches.

As will be shown, the avoidance of relativistic electron damage will be far more difficult in the nuclear than in the non-nuclear phase of ITER. This is due to the loss of control over the heating power and more importantly due to runaway seeding by the beta decay of tritium, which could result in 8 MA of relativistic electrons. The only significant seeding of electron runaway in the non-nuclear phase is from the remaining energetic electrons of the pre-thermal-quench Maxwellian. As will be discussed, this seed can be avoided in two ways: (1) by a sufficiently long time  $\tau_a$  for energetic electrons to cool between the initiation of the thermal quench and the Ohmic electric field exceeding the Connor-Hastie field for runaway, or (2) by all the magnetic surfaces opening and remaining open long enough  $\tau_{op}$  for even the energetic trapped electrons to cool. When these times are less than a few milliseconds at the standard ITER density, the full ITER current will be transferred to relativistic electrons; when these times are longer than approximately ten milliseconds essentially no current will be transferred. When the times  $\tau_a$  and  $\tau_{op}$  are significantly shorter than the current quench time, runaway due to tritium decay remains a problem.

Experiments on existing machines involving relativistic electrons have little direct relevance to ITER. Each drop of  $\approx 0.92$  MA during a quench in the plasma current increases the number of runaway electrons by an order of magnitude, so ITER at 15 MA can have fourteen orders of magnitude more increase than JET at 2 MA. To avoid halo currents, the 75 V·s of poloidal flux in ITER chamber must be removed within 150 ms, so the loop voltage must be greater than 500 Volts, more than hundred times the Connor-Hastie voltage for runaway. Skin currents associated with magnetic surface breakup could increase this voltage by an order of magnitude.

Experiments on existing machines are of critical importance for understanding what times  $\tau_a$  and  $\tau_{op}$  should be expected, the prevalence of skin currents, and the speed with which a plasma current can be terminated from an initial safety factor  $q$  without disrupting. Theory and modeling are essential. Gas-propelled pellets may take too long to reach the plasma if  $\tau_a$  and  $\tau_{op}$  are short. Passive breakup of the magnetic surfaces by currents induced in the walls by a disruption might prevent a runaway but has not been adequately investigated.

The status of work on current transfer has had ten-year markers since the danger first became apparent to the ITER management through the 1997 paper of Rosenbluth and Putvinski, *Theory for avalanche of runaway electrons in tokamaks* [2]. The Rosenbluth and Putvinski paper extended the work of Jayakumar, Fleischmann, and Zweben [3] on the exponentially large amplification of the number of energetic electrons through large-angle Coulomb collisions.

Ten years later, the 2007 *ITER physics basis document: chapter 3: MHD stability, operational limits and disruptions* [4] stated that ‘there is urgent need to clarify the properties of ‘disruption-generated’ runaway electrons and to establish methods for avalanche conversion avoidance and runaway discharge termination that can be reliably effected in an ITER-class tokamak’. The paper made predictions in table 5 on the

transfer of current to relativistic electrons. These results were largely based on the work of Rosenbluth and Putvinski, but Helander *et al* [5] was also referenced. The predicted amplification of the number of energetic electrons in [4] can be stated as

$$10^{|\delta I_p/I_{10}|}, \quad (1)$$

where  $\delta I_p$  is the change in the plasma current during the current quench and  $I_{10} \approx 0.92$  MA is the current change required for a ten-fold amplification in the number of energetic electrons. The current  $I_{10}$  has no intrinsic dependence on the plasma size but its magnitude has important uncertainties; both are discussed in section 3.2.

Twenty years later, the ITER Organization held a workshop on the disruption mitigation system (DMS) for ITER. The *Executive Report, ITER Disruption Mitigation Workshop, ITER HQ, 8–10 March 2017* [6] stated ‘A fully functional and effective DMS is essential for ITER to achieve its mission... The participants to this meeting... emphatically agree that immediate decisive action must be taken to directly support research into solutions to outstanding critical issues relating to the specification and performance of the DMS. The consensus is that significant uncertainties exist, in particular, as to whether the present baseline disruption mitigation system will offer sufficient protection to ITER from relativistic electron impacts’.

Research on the ‘outstanding critical issues’ presupposes a knowledge of what these issues are, but little has been published on what physics must be resolved to adequately protect ITER. In the absence of a definition of the critical issues and research foci, much of the research has focused on what is interesting and easily done rather than on what must be resolved.

The long history and the increasing rigidity of the ITER design raise concerns about a feasible solution being found even if a solution is in principle possible. These concerns are far greater in the nuclear than in the non-nuclear phase of ITER operations.

An important 2017 assessment of the present state of the physics was written by Martín-Solís with two senior scientists at the ITER Organization, M. Lehnen and A. Loarte, as co-authors: *Formation and termination of runaway beams in ITER disruptions* [7]. The authors described the paper as developing a ‘self-consistent analysis of the relevant physics regarding the formation and termination of runaway beams’ for ‘identifying open issues for developing and accessing disruption mitigation schemes for ITER’. The loss of magnetic surfaces was not considered by Martín-Solís *et al*, and the exponential sensitivities were considered only implicitly.

The information needed to protect ITER from unacceptable relativistic-electron damage cannot be obtained empirically—even on ITER: (1) Too large an extrapolation is required from existing tokamaks, such as JET. One of the most complete papers on natural thermal quenches in JET and in other tokamaks is a 2016 paper by de Vries *et al* [8]. Figure 1 from this paper illustrates a JET plasma that had a current before the thermal quench of  $I_{p0} = 1.3$  MA, figure 1. The required extrapolation

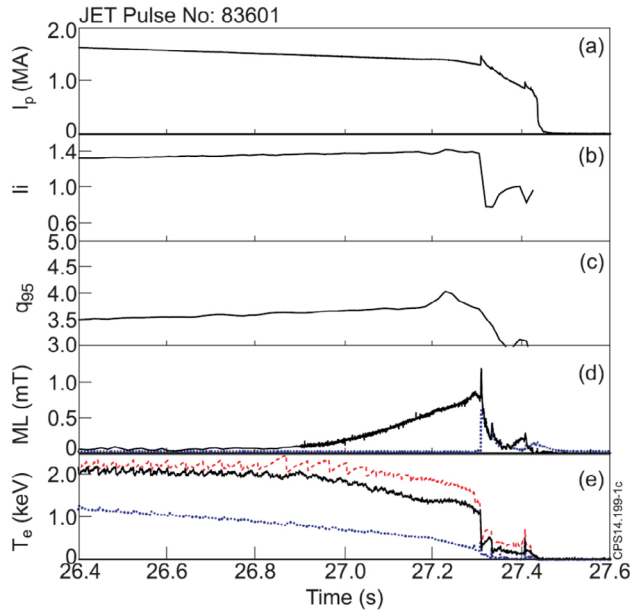


**Figure 1.** This is figure 1 from [8], which gave the evolution of a JET plasma into a natural thermal quench. Time traces are shown of (a) the plasma current  $I_p$ , (b) the internal inductance  $l_i$ , (c) the safety factor near the plasma edge  $q_{95}$ , (d) the magnitude of magnetic perturbations, which presumably open magnetic islands, and (e) the electron temperature at three radial positions in the plasma. Reproduced courtesy of IAEA. Figure from [8]. © 2016 EURATOM.

between that experiment and ITER at 15 MA is fifteen orders of magnitude in the expected amplification in the number of energetic electrons. (2) The potential for severe damage is too great for the use of ITER. Pulses that end with relativistic-electron damage could take months to repair. (3) The allowable rate of failure, of order once in a thousand pulses, would require too long to demonstrate. (4) The nuclear phase of ITER operations has an additional risk from relativistic electrons due to the beta decay of tritium.

Theory and simulations are also not sufficient: (1) The simulation of the fast breaking of magnetic surfaces is well beyond the capability of existing codes. (2) Although the exponential sensitivities could be calculated with far greater accuracy than they are at present, the uncertainties are too great for an adequate determination. Nevertheless, a far better assessment could be made of the implications of these uncertainties on the protection of ITER based on methods defined in this paper. An organized research program to determine what is going on in existing experiments during the thermal quench is desperately needed.

The two primary sections of the paper are section 2, which considers fast magnetic reconnection and magnetic surface breakup, and section 3, which considers the various exponential sensitivities that arise in the relativistic electron problem.

Boozer's paper *Runaway electrons and ITER* [1] had an extensive discussion of fast magnetic reconnection. As discussed in [1] fast magnetic reconnection (1) has an Alfvénic rather than a resistive time scale, (2) is a quasi-ideal process that conserves magnetic helicity, (3) can not itself accelerate electrons to high energies despite causing large changes in the dependence of poloidal flux on the toroidal flux, but (4) can

cause strong skin currents to arise that can greatly complicate the avoidance of relativistic electrons.

Unfortunately, a direct simulation of fast magnetic reconnection during ITER disruptions is well beyond present codes and computers [1]. In tokamak experiments, resistive transport of the poloidal magnetic flux relative to the toroidal flux, which can accelerate electrons to relativistic energies, is a competitive process to helicity-conserving fast magnetic reconnection. Section 2 on magnetic surface breakup explains how this competitive interaction can be studied using mean-field theory to impose the helicity-conservation constraint of Maxwell's equations, which was derived in [1]. As will be shown in appendix C, the change in the magnetic energy during a helicity-conserving relaxation in a tokamak can be very small, which makes the standard proof [9] that helicity is better conserved than magnetic energy of little relevance. Consequently, the helicity evolution equation, which was derived from Maxwell's equations in [1] is central to the arguments given in section 2 and in appendix A.

Exponential sensitivity of the transfer of current to relativistic electrons to the plasma state has been apparent for twenty years, but the discussion of the exponential dependence on  $\tau_a$  has been implicit and the exponential dependence on  $\tau_{op}$  as been ignored for decades. Each of these exponential dependencies has uncertainties, and a change by a factor of ten takes the answer from the full current to negligible current being transferred. It may well be possible to make  $\tau_a$  and  $\tau_{op}$  sufficiently long in the non-nuclear phase of ITER operations to avoid damage from runaways, but ensuring  $\tau_a$  and  $\tau_{op}$  are sufficiently long in the nuclear phase is far more demanding.

## 2. Magnetic surface breakup

The effect of large-scale islands destroying magnetic surfaces was ignored in the Rosenbluth–Putvinski [2] study of electron runaway for ITER as well as in many recent studies, such as the 2017 publications of Martín-Solís *et al* [7] and Aleynikov and Breizman [10]. Nevertheless, as will be discussed, experiments provide clear evidence that magnetic surface destruction is associated with thermal quenches, and simulations imply that surface breakup should occur. When magnetic surfaces are broken throughout the plasma for a time  $\tau_{op}$  that is sufficiently long, the transfer of the plasma current to relativistic passing electrons cannot occur because these electrons would strike the walls long before they have been accelerated to a relativistic energy. It will be difficult to provide convincing evidence that all surfaces are broken—even magnetic surfaces inside islands can be important [11]. When all magnetic surfaces are broken, not only is the time they remain open  $\tau_{op}$  important but also whether they re-form from the outside in or from the inside out [12].

The speed of thermal quenches implies the surface breaking must be due to a fast magnetic reconnection, which is a distinct physical process from the resistive diffusion of magnetic field lines. Although the direct simulation of fast magnetic reconnection is too demanding for existing codes and computers, realistic interpretations of existing experiments and

predictions for ITER require consideration of the effects of fast magnetic reconnection. This section will consider the effects of the breaking of magnetic surfaces on the formation of strong currents of relativistic electrons with a particular focus on how the effects of fast magnetic reconnection can be studied with a mean-field Ohm's law.

### 2.1. Fast magnetic reconnection

The current spike and the drop in the internal inductance, which frequently occur during thermal quenches, imply a large scale spreading of the current profile on an expected time scale of a millisecond in ITER [4]. The time scale is even faster in existing tokamaks. The only known way to spread the current density so quickly is by breaking the magnetic surfaces. The shortness of the timescale, far shorter than the Rutherford time [13] for the growth of islands in a hot plasma, implies the reconnection must be fast. Figure 1 shows the long timescale for the build up of non-axisymmetric magnetic perturbations in a natural disruption on JET compared to the time scale for the drop in the electron temperature and the internal inductance.

Fast magnetic reconnection has a rate determined by Alfvénic not resistive effects [14–16] and is prevalent in astrophysical, space, and laboratory plasmas [16]. Fast magnetic reconnection is a quasi-ideal process [1], which conserves magnetic helicity and cannot accelerate electrons to high energies despite large poloidal flux changes. The magnetic helicity in a region of space is the integral of the poloidal with respect to the toroidal magnetic flux,  $-2 \int \psi_p d\psi_t d\theta d\varphi / (2\pi)^2$ . The poloidal  $\psi_p$  and toroidal  $\psi_t$  fluxes as well as the poloidal and toroidal angles are defined in figure 2.

Most of the theory of fast magnetic reconnection is in artificial two-dimensional systems. In three dimensional systems, spatial scales as short as the electron inertial scale  $c/\omega_{pe}$  are required with a time scale set by the Alfvén wave [17, 18]. Nevertheless, effects that can be expected from fast magnetic reconnection must be understood if the dangers of relativistic electrons to ITER are to be assessed. There are three central questions: (1) Are essentially all confining magnetic surfaces destroyed? (2) Will strong surface currents in regions of confining surfaces but near their boundaries with stochastic magnetic field lines greatly enhance the difficulty of avoiding relativistic electrons? (3) How long is required for confining magnetic surfaces to re-form after their destruction?

Remarkably little experimental data has been published on current spikes and drops in the internal inductance though this data could be used to address questions that must be answered before a credible assessment can be made of the dangers to ITER of relativistic electrons.

### 2.2. Simulation of fast magnetic reconnection

Direct simulations of fast magnetic reconnection in ITER-like plasmas are not possible with existing codes and computers. Nevertheless, information can be obtained by a combination of theory and experiment. There are three ways to proceed

computationally: (1) The plasma resistivity can be artificially enhanced to whatever level is required to make a simulation feasible using codes such as NIMROD [19, 20] or JOREK [21, 22]. This suppresses fast magnetic reconnection and its effects. (2) Mean-field theory gives an essentially unique expression for local helicity transport [23],

$$\vec{E} \cdot \vec{B} = -\vec{\nabla} \cdot (\lambda \vec{\nabla} j_{\parallel} / B), \quad (2)$$

and this expression can be used as a sub-grid model [24] in a fully three-dimensional code such as M3D-C1 [25]. (3) A poloidal flux transport equation can be derived, appendix A, using the mean-field expression for the local helicity transport. This equation will be discussed in section 2.3.

The obvious difficulty with mean-field theory is obtaining an expression for the helicity transport coefficient  $\lambda$ , which relates the flux of magnetic helicity along the magnetic field lines  $\mathcal{F}_{\parallel}$  and the gradient of  $j_{\parallel}/B$ . The coefficient  $\lambda$  is zero in regions of confining magnetic surfaces and determined by an Alfvénic relaxation rate in regions in which the magnetic field lines are stochastic, equation (C.5). Experimental data on the drop in the internal inductance  $\ell_i$  and on current spikes can be used to determine  $\lambda$ . As will be shown, the fast rise of the current spike implies surfaces are broken in the outer part of the plasma—outside a magnetic surface that encloses a toroidal flux  $\psi_t = \psi_b$ . The time for the rise of the current spike and drop in  $\ell_i$  imply a value for  $\lambda$ . The change in the internal inductance  $\ell_i$  during the current spike determines a value for  $\psi_b$ . The magnitude of the current spike is then calculable. At least in machines the size of JET, the plasma resistivity must be included in the calculation of the current spike; resistive dissipation of helicity reduces the magnitude of the current spike below the level that would arise if the resistivity were zero.

When some magnetic surfaces are preserved throughout the thermal quench, a skin current will arise just inside the outermost magnetic surface,  $\psi_t = \psi_b$ , with a width and magnitude that can be calculated; an estimate is given in section 2.4. This skin current can greatly enhance the electron density required to avoid an exponential amplification of the number of energetic electrons from the values for the ‘ $n_e$  to suppress avalanche growth’ given in table 5 of [4].

Even a highly localized skin current can greatly enhance current transfer to relativistic electrons. Confined passing electrons anywhere in the plasma enclose a certain toroidal flux. As the poloidal flux outside that toroidal flux changes these electrons are accelerated and avalanche to relativistic energies [26]. When the current of the relativistic electrons is sufficiently large to sustain the poloidal flux, the electric field drops to approximately the Connor-Hastie value, which is required to maintain the relativistic current.

The requirement for a skin current follows from several basic points: (1) Magnetic field lines are the trajectories of a Hamiltonian  $\tilde{\psi}_p(\psi_t, \theta, \varphi)$ , appendix A, which is a Hamiltonian of the standard  $H(p, q, t)$  form. (2) When some trajectories of the Hamiltonian lie on perfect surfaces and some do not, then there is a distinct outermost confining surface, or Kolmogorov–Arnold–Moser (KAM) surface, that blocks trajectories from



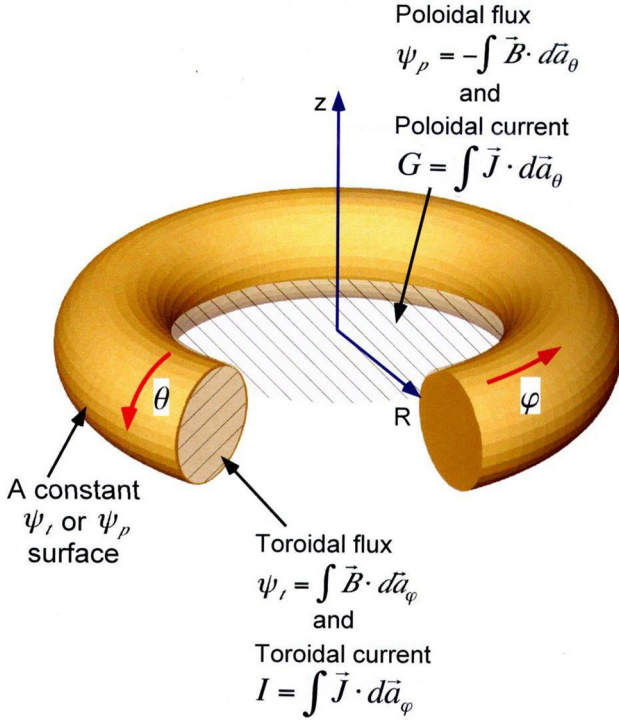


**Figure 2.** Two common coordinate systems for representing a torus are illustrated,  $(R, \varphi, Z)$  cylindrical coordinates and  $(\psi_t, \theta, \varphi)$  canonical coordinates of the magnetic field. The figure also defines the poloidal  $\psi_p$  and toroidal  $\psi_t$  magnetic fluxes as well as the poloidal  $G$  and toroidal  $I$  effective currents. In this paper, the effective current density  $\vec{J}$  equals the actual current density  $\vec{j}$ . Reproduced courtesy of IAEA. Figure from [36]. Copyright 2015 IAEA.

entering the region in which trajectories fill a volume rather than a surface [27]. (3) The radial flux of magnetic helicity along field lines  $\mathcal{F}_\parallel$  is blocked by this outermost KAM surface. Outside of this blocking surface, in the volume covered by a magnetic field line,  $\mathcal{F}_\parallel$  can transport helicity at an Alfvénic rate [1] to relax the gradient in  $j_\parallel/B$  while conserving the magnetic helicity,  $-2 \int \psi_p d\psi_t d\theta d\varphi / (2\pi)^2$ . (4) When resistive rates are negligibly small compared to the Alfvénic relaxation of the gradient of  $j_\parallel/B$  by  $\mathcal{F}_\parallel$ , the poloidal flux  $\psi_p$  is conserved as a function of the toroidal flux  $\psi_t$  in the region enclosed by the outermost KAM surface, the region in which  $\mathcal{F}_\parallel = 0$ , but only the magnetic helicity is conserved in the exterior region [1]. (5) The gradient of  $\psi_p$  gives the poloidal magnetic field, appendix A, so  $\psi_p$  must be continuous, but its gradient need not be and can not be continuous after  $j_\parallel/B$  has relaxed to a constant in the exterior region while conserving both  $\psi_p$  at the boundary and the magnetic helicity. (6) This jump in the poloidal field is equivalent to a surface current and must be within the region of confining magnetic surfaces, otherwise it would have been relaxed by  $\mathcal{F}_\parallel$ . (7) The width of the skin current, which is required to obtain the loop voltage it produces, depends on the square root of the ratio of the resistive diffusion time  $\tau_\eta$  and the Alfvénic relaxation time  $\tau_r$  for the gradient of  $j_\parallel/B$ , section 2.4. The Alfvénic relaxation time is longer than one might expect because the relaxation proceeds by wave propagation along volume-covering stochastic magnetic field lines, appendix C.

### 2.3. Mean-field equation for flux evolution

The mean-field equation for the poloidal flux evolution can be used to: (1) Provide mean  $\psi_p(\psi_t, t)$  information, which as will be seen in section 3.2 is required to determine both the magnitude and profile of the current transferred to relativistic electrons. (2) Find the expected number of energetic electrons, which could be compared with their presence or absence in experiments to clarify the extent in space and time of magnetic surface breaking. (3) Predict the existence of skin currents, which could greatly enhance the electron density required to avoid exponential amplification of the relativistic current. (4) Clarify the plasma state just before the re-formation of magnetic surfaces for use in a simulation of the re-formation (5) Determine what types of experimental measurements would best delineate how the plasma is evolving during a thermal quench.

If the mean-field equation for the poloidal flux evolution were embedded in an axisymmetric transport code, a linear analysis of the resistive stability of the plasma would be informative and could be carried out with far more limited computational requirements than for a full three dimensional analysis.

The mean-field evolution equation for the mean poloidal flux  $\psi_p(\psi_t, t)$ , which is derived in appendix A, is

$$\frac{\partial \psi_p(\psi_t, t)}{\partial t} = \mathcal{R}_\psi \frac{\partial I(\psi_t, t)}{\partial \psi_t} - \frac{\partial}{\partial \psi_t} \left( \psi_t \Lambda_m \frac{\partial^2 I}{\partial \psi_t^2} \right), \quad (3)$$

where the Ohmic resistance  $\mathcal{R}_\psi(\psi_t, t)$  is given by equation (A.11).  $\mathcal{R}_\psi$  is known when the temperature and  $Z_{\text{eff}}$  profiles are known. The helicity-conserving poloidal flux transport coefficient  $\Lambda_m(\psi_t, t)$  has a characteristic value, equation (C.5). The primary issue with  $\Lambda_m$  is whether it is zero, as it is where confining magnetic surfaces exist, or approximated by its characteristic value or the magnitude required to fit experiments, in regions in which magnetic field lines are stochastic. The poloidal  $\psi_p$  and toroidal  $\psi_t$  fluxes together with the enclosed toroidal current  $I$  are defined in figure 2.

The boundary condition required to solve this equation is the magnitude of the poloidal flux at the plasma edge, where the enclosed toroidal flux  $\psi_t = \Psi_t$ . For phenomena that are fast compared to the resistive time scale of the wall, such as thermal quenches, the edge value of the poloidal flux does not change, and  $\psi_p(\Psi_t)$  can be set to zero. When there is a loop voltage  $V_\ell$  at the plasma edge,  $\partial \psi_p(\Psi_t, t) / \partial t = V_\ell$ .

The poloidal flux and the current  $I$  are related at each point in time by

$$\psi_p(\psi_t) = - \int_{\psi_t}^{\Psi_t} \frac{L(\psi_t) I(\psi_t)}{2\psi_t} d\psi_t, \quad (4)$$

assuming  $\psi_p(\Psi_t) = 0$ . The poloidal flux  $\psi_p$  is negative at the magnetic axis,  $\psi_t = 0$ , when the plasma current is positive. Equation (4) follows from the definition the rotational transform  $\iota \equiv \partial \psi_p / \partial \psi_t$ , which is the inverse of the safety factor,  $q = 1/\iota$  and  $\iota = LI/2\psi_t$ , appendix B.1. The inductance

$$L(\psi_t) \equiv \frac{2\iota\psi_t}{I} \quad (5)$$

$$= \frac{2\kappa(\psi_t)}{1 + \kappa^2} \mu_0 R_0, \quad (6)$$

where the second form holds exactly for magnetic surfaces near the axis,  $\psi_t \rightarrow 0$ , which has a major radius  $R_0$  and with magnetic surfaces of elongation  $\kappa_0$ . Fast investigations can be made by assuming that the near-axis form for the inductance  $L_0 \equiv L(\psi_t \rightarrow 0)$  is accurate across the plasma and is independent of time. Otherwise, the poloidal flux evolution equation can be embedded in an axisymmetric transport code.

Equation (3) for the evolution of  $\psi_p$  and equation (4) for the relation between  $\psi_p$  and  $I$  can be used to obtain an equation for the evolution of the current,

$$\frac{\partial L I}{\partial t} = 2\psi_t \frac{\partial}{\partial \psi_t} \left( \mathcal{R}_\psi \frac{\partial I(\psi_t, t)}{\partial \psi_t} - \frac{\partial}{\partial \psi_t} \psi_t \Lambda_m \frac{\partial^2 I}{\partial \psi_t^2} \right). \quad (7)$$

An implication of equation (7) is that a spike in the total plasma current cannot occur faster than an edge resistive time scale unless  $\Lambda_m$  is non-zero all the way to the plasma edge. In principle, a large reduction in the inductance  $L$  by a change in the elongation  $\kappa$  could also increase the current, but for  $\kappa > 1$ , an unlikely large increase in  $\kappa$  would be required. The short time scale of current spikes in experiments implies that the magnetic field lines in the outer part of the plasma are rapidly made stochastic. An obvious model for the poloidal flux transport coefficient is  $\Lambda_m = 0$  when  $\psi_t < \psi_b$  and  $\Lambda = \Lambda_c$  when  $\psi_t > \psi_b$  after the start of the thermal quench, where  $\psi_b$  is the toroidal flux enclosed by the outermost confining magnetic surface and  $\Lambda_c$  is the characteristic value given in equation (C.5). The only undetermined parameter to which results are sensitive is  $\psi_b$ , which can be set by the internal inductance  $\ell_i$  after the current spike, equation (B.6).

#### 2.4. Skin-current estimate

The width of the skin current that arises on confining magnetic surfaces at their boundary with stochastic field lines can be estimated in an even simpler way than by the use of equation (7). The diffusion equation for the poloidal magnetic field is  $\partial B_p / \partial t = (\eta / \mu_0) \partial^2 B_p / \partial x^2$ , which has the solution  $\delta B_p(t) = \delta B_0 \exp(t/\tau_r) \exp(-|kx|)$  for the jump in the poloidal field across the boundary between confining surfaces and the stochastic magnetic field lines. The time  $\tau_r$  is the time required for that jump in the poloidal field to arise and is the time scale of a fast magnetic reconnection  $\tau_r \sim 1$  ms. The spatial scale of the skin current is  $1/k = \sqrt{\eta \tau_r / \mu_0}$ . The current density of the skin current is  $j_s = (\partial \delta B_p / \partial x) / \mu_0$ , so the skin current is

$$j_s = \left( \frac{\delta B_p}{\mu_0 a} \right) \sqrt{\frac{\tau_r}{\eta}}, \quad (8)$$

where  $a$  is the plasma radius and  $\tau_\eta = \mu_0 a^2 / \eta$  is the global resistive time scale. A characteristic resistive time scale is  $\tau_\eta \approx 150$  ms, which is the time scale during which the plasma will drift into the wall when axisymmetric equilibrium is lost; the current must be removed on this time scale to avoid a halo current. This gives a current density in the skin current, which

is an order of magnitude greater than the average current density in the plasma.

#### 2.5. Re-formation of magnetic surfaces

If the stochastic magnetic field regions, the current profile, the temperature profile, and  $Z_{\text{eff}}$  profiles were known after the thermal quench, then three-dimensional codes, such as NIMROD, JOEREK, or M3D-C1, could determine how quickly confining magnetic surfaces re-form—particularly outer magnetic surfaces. Indeed, the re-formation of magnetic surfaces has been seen in NIMROD [19, 20] and JOEREK [21, 22] simulations of thermal quenches. The resistivity is sufficiently high in post-thermal-quench plasmas that simulations of the re-formation of surfaces can be realistically made—unlike the situation at the beginning of the thermal quench.

The realism of the simulations of the re-formation of surfaces is limited by the accuracy with which the regions of stochastic magnetic field lines and the current profiles are known. The mean-field equation for poloidal flux transport could be used together with experimental data to clarify the plasma state just before the re-formation of magnetic surfaces.

A particularly important issue is whether outer magnetic surfaces re-form first. Even a narrow annulus of magnetic surfaces will prevent the escape of energetic electrons, which have a small gyroradius compared to system size in ITER. Boozer and Punjabi [12] have used the Hamiltonian mechanics concept of turnstiles [28] to show that relativistic electrons confined in a large region of stochastic magnetic field lines by a narrow annulus of magnetic surfaces are prone to fast, extremely concentrated depositions on the surrounding walls.

### 3. Exponential sensitivities

#### 3.1. Estimate of relativistic current

The seriousness of the transfer of the pre-disruption plasma current  $I_{p0}$  to relativistic electrons is largely determined by the magnitude the transferred current  $I_{\text{rel}}$ .

The exponential amplification  $10^{|\delta I_p / I_{p0}|}$  of the number of seed electrons was discussed in the introduction and will be considered in section 3.2.

The initial number density of energetic electrons  $n_s$ , called seed electrons, which are available to be amplified, will also be found to be exponentially dependent on parameters. That is,

$$n_s = 10^{-\ell_{\text{seed}}} n_0, \quad (9)$$

where  $n_0$  is the pre-disruption electron number density and  $\ell_{\text{seed}}$  is calculated in sections 3.3 and 3.4. Note that a large  $\ell_{\text{seed}}$  means there are few seed electrons.

The current density of relativistic electrons moving parallel to the magnetic field is  $j_{\text{rel}} \approx en_{\text{rel}}c$ . For this current density to equal the pre-disruption current density in ITER, a certain number of relativistic electrons are required,

$$n_{\text{rel}} = 10^{-\ell_{\text{req}}} n_0, \quad (10)$$

where  $\ell_{\text{req}} \approx 3.7$ .

The relativistic current that results from the avalanche is

$$I_{\text{rel}} = I_{p0} 10^{-(\ell_{\text{seed}} - \ell_{\text{req}})} 10^{(I_{p0} - I_{\text{rel}})/I_{10}}, \text{ so} \quad (11)$$

$$I_{\text{rel}} = I_{p0} - \left( \ell_{\text{seed}} - \ell_{\text{req}} - \log_{10} \frac{I_{p0}}{I_{\text{rel}}} \right) I_{10} \quad (12)$$

$$\approx I_{p0} - (\ell_{\text{seed}} - \ell_{\text{req}}) I_{10}, \quad (13)$$

for the logarithmic term,  $\log_{10}(I_{p0}/I_{\text{rel}})$ , is rarely of major importance. As noted in the Introduction  $I_{10} \approx 0.92$  MA in the standard calculation [4] independent of the size of the machine.

Equation (13) has three cases: (1) The large-seed case,  $\ell_{\text{seed}} - \ell_{\text{req}} \ll I_{p0}/I_{10}$ , in which essentially the full plasma current is transferred to relativistic electrons. (2) The intermediate-seed case,  $\ell_{\text{seed}} - \ell_{\text{req}} \sim I_{p0}/I_{10}$ , in which the relativistic current is smaller than the initial plasma current but still substantial. (3) The small-seed case,  $\ell_{\text{seed}} - \ell_{\text{req}} \gg I_{p0}/I_{10}$ , in which the relativistic current is exponentially small compared to the plasma current. Using Equation (11),  $I_{\text{rel}} \approx I_{p0} 10^{-\ell}$ , where  $\ell \equiv \ell_{\text{seed}} - \ell_{\text{req}} - \ell_{p0}/\ell_{10}$  using equation (12).

The intermediate-seed case,  $\ell_{\text{seed}} - \ell_{\text{req}} \sim I_{p0}/I_{10}$ , or  $\ell_{\text{seed}} \sim 20$ , is the only one that requires careful analysis. For this case even a factor of two in either  $I_{10}$  or  $\ell_{\text{seed}}$  can make a dramatic difference in the danger of relativistic electrons to ITER.

### 3.2. Exponentiation of energetic electrons

Although the exponentiation in the number of energetic electrons is customarily expressed in terms of the change in the plasma current, it is actually determined by the change in the poloidal flux. There are four uncertainties: (1) an overall coefficient  $\gamma_{\text{ef}}/\ln \Lambda$ , (2) the Coulomb logarithm  $\ln \Lambda$ , (3) the plasma flux inductance  $\mathcal{L}$ , and (4) the profile of the change in the poloidal flux. Each of these four uncertainties will be discussed.

The coefficient  $\gamma_{\text{ef}}/\ln \Lambda$  is a dimensionless ratio giving the relative strength of small-angle collisions, which give the collisional drag that limits electron runaway and depend on the Coulomb logarithm,  $\ln \Lambda$ , and the large-angle collisions, which determine the rate of scattering of cold electrons to high energy and do not depend on  $\ln \Lambda$ . The dimensionless coefficient  $\gamma_{\text{ef}}$  is important not only for determining the poloidal flux change required for an e-fold but also for determining the energy distribution of energetic electrons. When the exponentiation is the only non-ideal effect on high energy electrons, the resulting pitch-angle-averaged distribution function of relativistic electrons is [1]

$$f(p, t) = \frac{\exp(-p/p_0)}{p_0 p^2} n_e(t=0) \exp\left(\frac{|\delta\psi_p|}{\gamma_{\text{ef}} \psi_{\text{pa}}}\right), \quad (14)$$

where the momentum  $p = \gamma mc$  and  $p_0 = \gamma_{\text{ef}} mc$ , with  $\gamma$  the relativistic gamma factor [1].

**3.2.1. Flux change required for an e-fold.** The best known exponentiation is in the number of energetic electrons, which is essentially the exponentiation of the current density carried by relativistic electrons  $j_r$ . The basic formula, which was given by Rosenbluth and Putvinski [2], is

$$\frac{1}{j_r} \frac{dj_r}{dt} = \frac{1}{2 \ln \Lambda} \frac{eE_{\parallel}}{m_e c}, \quad (15)$$

when the parallel electric field  $E_{\parallel}$  is far larger than the Connor-Hastie field [29]

$$E_{\text{ch}} = 4\pi r_e^2 n_b \frac{m_e c^2}{e} \ln(\Lambda), \quad (16)$$

where  $r_e \equiv (e^2/m_e c^2)/(4\pi\epsilon_0)$  is the classical electron radius. The maximum Coulomb drag force that background electrons of density  $n_b$  exert on an energetic electron is  $eE_{\text{ch}}$ .

Equation (15) was derived ignoring pitch-angle scattering. Helander *et al* [5] replaced the  $2 \ln \Lambda$  in equation (15) by  $3\sqrt{2/\pi} \ln \Lambda \approx 2.39 \ln \Lambda$  for a hydrogenic plasma including the effect of pitch-angle scattering.

Appendix A of [26] shows that when magnetic surfaces exist, the accelerating passing electrons are essentially tied to the magnetic surfaces that enclose a fixed toroidal flux, and the accelerating electric field is essentially related to the time rate of change of the poloidal magnetic flux outside of that surface, which is the loop voltage,  $V_{\ell} \equiv \partial\psi_p(\psi_t, t)/\partial t \approx 2\pi R_0 E_{\parallel}$ , where  $R_0$  is the major radius. Therefore, the Rosenbluth–Putvinski expression of equation (15) is equivalent to

$$\frac{1}{j_r} \left( \frac{\partial j_r}{\partial t} \right)_{\psi_t} = \frac{1}{2\psi_{\text{pa}} \ln \Lambda} \left( \frac{\partial \psi_p}{\partial t} \right)_{\psi_t}, \quad (17)$$

$$\psi_{\text{pa}} \equiv 2\pi R_0 \frac{m_e c}{e}. \quad (18)$$

For  $R_0 = 6.2$  m, which is the major radius of ITER,  $\psi_{\text{pa}} \approx 0.0664$  V · s. A change in the poloidal flux by  $\psi_{\text{pa}}$  changes the kinetic energy of a passing, collisionless electron by  $m_e c^2$ .

The number of energetic electrons e-folds each time the poloidal flux changes by

$$\psi_{\text{ef}} = \gamma_{\text{ef}} \psi_{\text{pa}}, \text{ where} \quad (19)$$

$$\gamma_{\text{ef}} = 2.39 \ln \Lambda \quad (20)$$

when the Helander *et al* [5] expression for the exponentiation is used. Rosenbluth and Putvinski [2] showed that effects such as the pitch-angle scattering of high atomic number impurities could substantially reduce the exponentiation, which is equivalent to enhancing the dimensionless coefficient  $\gamma_{\text{ef}}$ .

**3.2.2. Characteristic voltages and runaway energy.** At the standard ITER electron density,  $n_b = 10^{20} \text{ m}^{-3}$ , the Connor-Hastie voltage  $V_{\text{ch}} \equiv 2\pi R_0 E_{\text{ch}} \approx 2.9$  V. The loop voltage required to remove the poloidal magnetic flux between the magnetic axis and the wall in ITER,  $\Psi_p \approx 75$  V · s, in the drift time of the plasma into the walls  $\approx 150$  ms is  $V_{\ell} \approx 500$  V.



The kinetic energy that an electron must have to runaway is  $K_r \approx (V_{ch}/V_\ell)m_e c^2 \sim 3$  keV, far below the thermal energy in the pre-thermal-quench Maxwellian.

At 10 keV, the parallel resistivity of a hydrogenic plasma is  $\eta = 0.65 \times 10^{-9}$  Ohm·m. The typical current density in ITER is  $1 \text{ MA m}^{-2}$ . The loop voltage  $V_\ell = 2\pi R_0 \eta j$  has the characteristic value during standard operations of  $2.5 \times 10^{-2}$  V. Since  $\eta \propto 1/T^{3/2}$ , the plasma temperature must be below 500 eV to exceed the Connor-Hastie voltage and approximately 14 eV to remove the poloidal flux in 150 ms.

**3.2.3. Coulomb logarithm.** The Coulomb logarithm is not extensively discussed in the literature. Rosenbluth and Putvinski [2] on page 1358 gave an expression  $\ln \Lambda \approx 18 + \ln |p/m_e c|$ , where  $p$  is the momentum of the high energy electron;  $p/m_e c = \sqrt{2K/m_e c^2}$  for a non-relativistic electron with kinetic energy  $K$ . For exponentiation, the critical kinetic energy is the kinetic energy required for runaway  $K_r \approx (E_{ch}/E_\parallel)m_e c^2$ , which is typically a few kilovolts. The Rosenbluth–Putvinski value is then  $\ln \Lambda \approx 16$ .

Rosenbluth and Putvinski also noted that when the electron being scattered has an energy far above that of the tightest-bound electrons in the ions, even electrons bound in ions contribute to  $n_b$ , and  $Z$  should be the atomic number of the nucleus and not just the ionization state of the ion. The Coulomb logarithm is reduced by a factor of approximately two for bound relative to free electrons. Any reduction in the Coulomb logarithm reduces the change in current  $I_{10}$  required to increase the number of energetic electrons by a factor of ten and increases the danger of a large transfer of current to relativistic electrons.

Solodov and Betti [30] derived a Coulomb logarithm for the stopping of electrons with kinetic energy  $K$  by cold electrons,

$$\ln \Lambda = \ln \left( \frac{K}{\hbar \omega_{pe}} \right). \quad (21)$$

Their equation (11) for the drag on an energetic electron is tricky because the expression in front of the logarithm differs by a factor of two from the conventional expression. Using the standard ITER density,  $10^{20} \text{ m}^{-3}$ , the Solodov and Betti expression gives  $\ln \Lambda \approx 15$ .

Even ignoring the bound electron effect, these two estimates of  $\ln \Lambda$  significantly increase the relativistic electron danger from conventional estimates [4] using  $\ln \Lambda \approx 20$ . That is  $I_{10} = 0.7 \text{ MA}$  may be a more accurate estimate.

**3.2.4. Current required for an e-fold.** The exponentiation in the number of runaway electrons is due to the change in the poloidal flux, but it is customary to express this by the change in the plasma current. The reason is that, unlike the flux change, the change in the plasma current required for an e-fold in the number of energetic electrons has no explicit dependence on the plasma size.

Letting  $\Psi_p$  be the poloidal flux enclosed by the axis, the maximum number of exponentiations is  $|\Psi_p/\gamma_{ef}\psi_{pa}|$ . Rosenbluth and Putvinski expressed this in a form equivalent

to  $2I_{p0}/\gamma_{ef}I_A$ , where  $I_{p0}$  is the pre-disruption plasma current and  $I_A = m_e c^3/e$  is the Alfvén current in Gaussian units. In the international system of units (SI), which are used in this paper, the Alfvén current is  $I_A = 4\pi\epsilon_0 m_e c^3/e \approx 17 \text{ kA}$ . The characteristic inductance of a toroidal plasma is  $L_c = \mu_0 R_0$ , where  $R_0$  is the major radius, and the poloidal flux change required to impart momentum  $m_e c$  to an electron is  $\psi_{pa} = 2\pi R_0 m_e c/e$ , so

$$I_A = 2 \frac{\psi_{pa}}{L_c}. \quad (22)$$

There are different plasma inductances. For example, one gives the relation between magnetic field energy and current squared and another between poloidal flux and plasma current, but all are the characteristic inductance  $L_c$  times a factor that depends on the current profile and logarithmically on the aspect ratio of the plasma. Their linear dependence on  $R_0$  is essentially obvious from figure 2. The inductance of importance to electron runaway relates the change in the poloidal flux enclosed by the axis produced by a change in the plasma current,

$$\mathcal{L} \equiv \frac{|\delta\Psi_p|}{|\delta I_p|}. \quad (23)$$

The change in the plasma current  $I_{ef}$  required for an e-fold increase in the number of runaway electrons and the change for a factor of ten increase are

$$\left| \frac{\delta I_p}{I_{ef}} \right| \equiv \left| \frac{\delta\Psi_p}{\gamma_{ef}\psi_{pa}} \right| \text{ so} \quad (24)$$

$$I_{ef} = \frac{\gamma_{ef}}{2} \frac{\mu_0 R_0}{\mathcal{L}} I_A \text{ and} \quad (25)$$

$$I_{10} = \ln(10) I_{ef} \approx 2.30 I_{ef}. \quad (26)$$

The estimate  $I_{10} = 0.92 \text{ MA}$ , which is consistent with the exponentiation given in [4], corresponds to  $\ln \Lambda = 19.7$  when  $\mathcal{L} = L_c$ .

**3.2.5. Flux inductance.** The flux inductance  $\mathcal{L}$  can be significantly smaller than  $L_c \equiv \mu_0 R_0$  for standard current profiles and for shaped plasmas. In appendix B.2.1, the flux inductance for a flattop current profile is found to be

$$\mathcal{L} = L_0 \frac{1 + 2\ell_p}{4}; \quad (27)$$

$$L_0 = \frac{2\kappa_0}{1 + \kappa_0^2} \mu_0 R_0; \quad (28)$$

$$\ell_i = \frac{2\kappa_0}{1 + \kappa_0^2} \ell_p, \quad (29)$$

where  $\kappa_0$  is the elongation of the magnetic surface, which is assumed to be constant across the plasma, and  $\ell_p$  is the internal inductance calculated as if the plasma had circular surfaces and  $\ell_i$  is the actual internal inductance. Typically  $3/2 > \ell_p > 1/2$ , so  $1 > (1 + 2\ell_p)/4 > 1/2$ . For a typical ITER elongation,  $\kappa_0 = 1.85$ , the shaping factor

$2\kappa_0/(1 + \kappa_0^2) = 0.84$ . When  $\mu_0 R_0/\mathcal{L}$  is greater than one, the current  $I_{10}$  is proportionately increased, which reduces the danger from relativistic electrons for a plasma of given current. Nevertheless, the damage that can be done by a single incident of a strong relativistic electron current striking the walls is so great that it is not the typical case but the most dangerous credible case that is important.

**3.2.6. Flux change profile.** The poloidal flux enclosed by the magnetic axis has a larger magnitude  $|\Psi_p|$  than at any other location in the plasma—a factor of two greater than at a typical point in the plasma. The estimates of the relativistic current of section 3.1 may have a factor of two error due to profile effects. To obtain more accurate values for the relativistic current and its profile, the evolution of the poloidal flux must be followed using equations such as those of section 2.3. When the magnetic surfaces remain perfectly intact, this is essentially the study made by Smith *et al* [31], which found that as the current is transferred to relativistic electrons the current density becomes centrally peaked.

The current spike and internal inductance drop that arise in association with the thermal quench imply that at least the outer magnetic surfaces are broken. The effect on the magnitude and profile of the relativistic current can be studied, including the effect of skin currents, using the transport coefficient  $\Lambda_m$  with the constraint that no runaway electrons are confined when  $\Lambda_m > 0$  all the way to the plasma edge. An even more peaked profile should be obtained than that found by Smith *et al* [31]. The stability of the resulting current profiles to ideal kinking or resistive tearing is questionable and could be investigated using both linear codes and fully non-linear three-dimensional MHD codes, which have adequate resolution to study the cold post-thermal quench plasmas.

### 3.3. Exponential loss of hot-Maxwellian seed

Potentially the strongest source of seed electrons is electrons remaining from the pre-thermal-quench Maxwellian. Since essentially all of the electrons in this Maxwellian are above the critical energy for runaway, the strength of this seed is determined by the fraction that remain energetic until they can be accelerated by the loop voltage. There are two mechanisms that may eliminate this seed: (1) Energetic electrons from the hot Maxwellian may be cooled before the loop voltage is sufficiently large to exceed the collisional drag force on these electrons. (2) Passing energetic electrons will quickly strike the walls when all confining magnetic surfaces are broken. Even then, the trapped electrons do not leave the plasma and can serve as a seed [32] when a sufficient number remain trapped and energetic during the time  $\tau_{op}$  in which all of the magnetic field lines are open.

The collision operator for non-relativistic electrons with an energy far above the thermal energy can be obtained from an expression given by Karney and Fisch [33],

$$\frac{\partial f}{\partial t} = \nu_{ch} \frac{c^3}{v^2} \frac{\partial f}{\partial v} + \frac{(1+Z)\nu_{ch}}{2} \frac{c^3}{v^3} \frac{\partial}{\partial \lambda} (1 - \lambda^2) \frac{\partial f}{\partial \lambda} \quad (30)$$

$$\nu_{ch} \equiv \frac{eE_{ch}}{mc} \approx \frac{1}{23 \text{ ms}} \frac{n_b}{10^{20} \text{ m}^{-3}}, \quad (31)$$

$$\begin{aligned} \nu_h &\equiv \nu_{ch} \left( \frac{mc^2}{T_h} \right)^{3/2} \\ &\approx \frac{1}{62 \mu\text{s}} \left( \frac{10 \text{ keV}}{T_h} \right)^{3/2} \frac{n_b}{10^{20} \text{ m}^{-3}}, \end{aligned} \quad (32)$$

$\lambda \equiv v_{||}/v$ , the effective charge state of the ions is  $Z$ , and the density of the cold background electrons is  $n_b$ .

**3.3.1. Maxwellian seed from passing electrons.** When some magnetic field lines lie in flux tubes that never intercept the walls, the passing electrons from the pre-thermal-quench Maxwellian can form a seed when they are not slowed by Coulomb collisions before the parallel electric field  $E_{||}$  is sufficiently strong to overcome the Coulomb drag. The time scale for  $eE_{||}$  acceleration to overcome the drag is approximately  $\tau_a$ , the time between the beginning of thermal quench and the time at which  $E_{||}$  exceeds  $E_{ch}$ .

When the plasma purity is unchanged during the thermal quench, it will be shown that passing Maxwellian electrons produce a seed

$$\ell_{seed} \approx \frac{1}{\ln(10)} \left( \frac{3}{2\sqrt{2}} \nu_h \tau_a \right)^{2/3}, \quad (33)$$

where  $\nu_h$  is the electron–electron collision frequency of the Maxwellian before the thermal quench. Impurities increase the collision frequency. Remember, the larger  $\ell_{seed}$  the fewer seed electrons, equation (9). The danger to ITER from runaways is most sensitive to the value of  $\ell_{seed}$  when  $\ell_{seed} \sim 20$ , which is equivalent to  $\nu_h \tau_a \sim 90$  or  $\tau_a \sim 6$  ms for a typical ITER collision frequency, equation (32). A factor of three change in  $\nu_h \tau_a$  from ninety would fundamentally change the danger to ITER from relativistic electrons.

There are four primary points related to the sensitivity to  $\nu_h \tau_a$ : (1) The total temperature drop during a thermal quench on ITER will be roughly a factor of a thousand. The temperature need only decrease by an amount comparable to the square root of a thousand for  $\eta j_{||}$  to exceed  $E_{ch}$ . The cooling processes during this part of the drop in the temperature may well be quite different than in the second part. Experimental data exists that could clarify the temperature evolution during the thermal quench, figure 1. (2) Impurities affect  $E_{ch}$  and the effective  $\nu_h$ . The charge state of impurities affects  $\eta$ . Data on impurities may exist. (3) A large change in the current density  $j_{||}$  may occur during the thermal quench due to the formation of a skin current, which could significantly reduce  $\tau_a$ . (4) The largest uncertainty is the extent to which confining magnetic surfaces persist during the thermal quench.

The strength of the seed from passing electrons can be estimated by noting that the Fokker–Planck equation for non-relativistic electrons that are highly super-thermal and isotropic is

$$\frac{\partial \bar{f}}{\partial t} = \frac{1}{v^2} \frac{\partial}{\partial v} (v^3 \nu(v) \bar{f}), \quad (34)$$

where  $\bar{f}$  is the average of  $f$  over  $\lambda$ , the collision frequency  $\nu(v) = \nu_h(T_h/mv^2)^{3/2}$ . To find the loss of energy of electrons that have an initial energy  $K_0 = mv_0^2/2$ , consider  $\bar{f}(v) \propto \delta(v - v_0)$ , and calculate the relation between  $dK/dt = \int (mv^2/2)(\partial f/\partial t)4\pi v^2 dv$  and  $K$ . The lowest energy electron that can be accelerated before it loses all of its energy is

$$K_a = \left( \frac{3}{2\sqrt{2}} \nu_h \tau_a \right)^{2/3} T_h. \quad (35)$$

The fraction of passing electrons in the pre-thermal-quench Maxwellian that are passing and have an energy above  $K_a$  is approximately  $\exp(-K_a/T_h)$ , so

$$\begin{aligned} n_e(0) &\approx n_0 \exp \left( - \left( \frac{3}{2\sqrt{2}} \nu_h \tau_a \right)^{2/3} \right) \\ &\approx n_0 \exp \left( - (1.061 \nu_h \tau_a)^{2/3} \right). \end{aligned} \quad (36)$$

When accelerated to the speed of light, approximately  $2 \times 10^{-4} \approx 10^{-3.7} \approx e^{-8.5}$  of the electron density  $10^{20} \text{ m}^{-3}$  is required to carry a current density of  $1 \text{ MA m}^{-2}$ , a typical current density for ITER. There are this many hot-tail electrons when  $\nu_h \tau_a \lesssim 23$ , which for standard ITER conditions of  $n_b = 10^{20}/\text{m}^3$  and  $T_h = 10 \text{ keV}$  corresponds to  $\tau_a \lesssim 1.35 \text{ ms}$ .

The seed that arises from tritium decay will be found to have a strength of  $n_s \approx 3 \times 10^{-12} n_0 \approx e^{-26.5} n_0$ . The hot-Maxwellian tail is a stronger seed when  $\nu_h \tau_a \lesssim 127$ , or  $\tau_a \lesssim 8 \text{ ms}$ .

When the initial plasma current is  $15 \text{ MA}$  and the final runaway current is at least  $3 \text{ MA}$ , the avalanche exponentiation can be  $10^{13}$  and an initial runaway seed of only  $10^{-16.7} n_0$  is required, which implies  $\nu_h \tau_a \lesssim 212$ , or  $\tau_a \lesssim 13 \text{ ms}$ .

A calculation of the source of seed electrons has been made by Smith and Verwichte [34] assuming the cooling is exponential and by Alenikov and Breizman [10] who studied the thermal quench including radiative cooling by impurities. What is clear is that the details of the early cooling are of exponentially great importance. They may not be adequately represented by the overall thermal quench time nor by radiative cooling calculation due to the uncertainties in the impurity profiles and charge states.

The cooling along open magnetic field lines can be very rapid, but the transfer of the current to relativistic electrons can only occur in regions in which the magnetic field lines do not intercept the walls. The thermal transport across the boundary between confined and open lines can be large, maybe Bohm-like  $D \sim T/eB$ , and shorten  $\tau_a$ .

At a typical ITER current density of  $1 \text{ MA m}^{-2}$ , an electron temperature  $T_{\text{ch}} \approx 500 \text{ eV}$  is required for the loop voltage to exceed the Connor-Hastie voltage in a hydrogenic plasma. However, skin currents naturally arise near the surface that separates confined and unconfined magnetic field lines, section 2.4. Within these layers the current density could be an order of magnitude greater. An order of magnitude increase in the current density could raise the critical temperature for runaway to  $T_{\text{ch}} \approx 2 \text{ keV}$ .

Experimental determinations of  $\tau_a$  could be made. As illustrated in figure 1, temperature measurements can be made during the thermal quench, and some data exists on the impurities and their charge states in order to calculate the collision frequency. Such studies are required to determine the credibility of extrapolations to ITER.

The largest uncertainty appears to be the extent to which confining magnetic surfaces remain throughout the thermal quench. A current transfer to relativistic electrons can occur on stochastic field lines in a region bounded by a confining magnetic surface. Such a situation arises in the early part of a simulation of central injection of impurities into DIII-D [35].

**3.3.2. Maxwellian seed with temporary loss of surfaces.** When the beginning of the thermal quench corresponds to the loss of all confining magnetic surfaces, the energetic passing electrons escape too rapidly to form a seed. Nevertheless, as noted by Fleischmann and Zweben [32], energetic trapped electrons are only lost when they are either cooled or collisionally detrapped and can provide a seed when some confining magnetic surfaces re-form within a time  $\tau_{\text{op}}$ . The importance of this seed does not appear to be recognized in the ITER literature.

The strength of this source can be estimated by considering the pitch-angle dependent part of the distribution function  $f_\lambda(\lambda, t)$  for trapped electrons. The  $\lambda$  dependence can be modeled by the self-similar solution to the equation for pitch angle scattering,  $f_\lambda \propto \cos((\pi/2)\lambda/\lambda_t)$ , where  $|\lambda_t| = \sqrt{2\epsilon} \ll 1$  is the maximum pitch at which an electron can be trapped and  $\epsilon$  is the local inverse aspect ratio. The kinetic equation for  $f_\lambda$  is then

$$\frac{\partial f_\lambda}{\partial t} = -\nu_\lambda \left( \frac{T_h}{K} \right)^{3/2} f_\lambda; \quad (37)$$

$$\nu_\lambda \equiv \frac{(\pi/2)^2}{2^{7/2}\epsilon} (1+Z)\nu_h \approx 0.218 \frac{1+Z}{\epsilon} \nu_h. \quad (38)$$

The fraction of the electrons of kinetic energy  $K$  that remain trapped during the time  $\tau_{\text{op}}$  decreases exponentially as  $\nu_\lambda \tau_{\text{op}} (T_h/K)^{3/2}$ .

Ignoring the loss of kinetic energy by collisional drag, the fraction of trapped electrons that remain after the time  $\tau_{\text{op}}$  is  $\exp(-K/T_h - \nu_\lambda \tau_{\text{op}} (T_h/K)^{3/2})$ . The kinetic energy that maximizes this fraction is

$$\frac{K_m}{T_h} = \left( \frac{3}{2} \nu_\lambda \tau_{\text{op}} \right)^{2/5} \quad (39)$$

$$\approx \left( 0.327 \frac{1+Z}{\epsilon} \nu_h \tau_{\text{op}} \right)^{2/5}. \quad (40)$$

The number of seed electrons is approximately

$$n_e(0) \approx n_0 \exp \left( - \left( 1.173 \frac{1+Z}{\epsilon} \nu_h \tau_{\text{op}} \right)^{2/5} \right). \quad (41)$$

This approximation is valid only when  $K_m/T_h$  is sufficiently large that the optimal electrons have not lost their energy

first. Presumably the time  $\tau_a$  is very short on open magnetic field lines,  $\tau_a \ll \tau_{op}$ , so electrons can be accelerated as soon as confining magnetic surfaces have formed. Therefore equation (41) is valid when

$$\frac{K_m}{T_h} > (1.061\nu_h\tau_{op})^{2/3}, \text{ or} \quad (42)$$

$$\nu_h\tau_{op} < 0.279 \left( \frac{1+Z}{\epsilon} \right)^{3/2}. \quad (43)$$

Otherwise the cooling of the energetic electrons during the time  $\tau_{op}$  dominates, and

$$n_e(0) \approx n_0 \exp \left( - (1.061\nu_h\tau_{op})^{2/3} \right). \quad (44)$$

It seems unlikely that  $\tau_{op}$  is sufficiently short to satisfy the inequality, so the seed from trapped electrons is generally given by equation (44). Consequently the strength of the trapped electron seed is essentially identical to the hot-tail seed in non-intercepting flux tubes but with  $\tau_a$  replaced by  $\tau_{op}$ .

Trapped electrons have an additional loss process. They can drift across the plasma and be lost, but this appears to be too slow to be relevant. The approximate radial drift velocity of a trapped electron moving with a speed  $v$  when the non-axisymmetric part of the magnetic field has the form  $B = B_0(1 - \delta \sin(N\varphi - M\theta))$  is

$$V_r = M\delta \frac{\rho}{2r} v \cos(N\varphi - M\theta), \quad (45)$$

where  $\rho$  is the gyroradius and  $r$  is the local minor radius. For a 100 keV electron this radial velocity is  $V_r \approx 3M\delta$  m ms<sup>-1</sup>. The time required for a trapped electron to cross a plasma of minor radius  $a$  is significantly longer than  $a/V_r$  because the complexities of the non-axisymmetric field will generally change the sign of  $V_r$  during the drift motion.

What is clear from this analysis is that the time until some confining magnetic surfaces re-form,  $\tau_{op}$  is extremely important. Simulations using JOEKE and NIMROD can provide some information, but it is also important to analyze experiments for evidence for the re-formation of confining surfaces.

### 3.4. Weak sources of seed electrons

Tritium decay and Compton scattering of electrons by gamma rays emitted by the walls can provide weak sources of seed electrons. They are only relevant when the exponential reduction in the number of seed electrons from the pre-thermal-quench Maxwellian is extremely large and are only present when ITER is in a nuclear phase. Nevertheless, they could then be important when the time  $\tau_a$  for the rise in  $E_{||}$  to  $E_{ch}$  or the time the magnetic surfaces stay open  $\tau_{op}$  are long. Even then sufficient poloidal flux must remain after confining surfaces re-form to allow a large number of exponentiations, which implies  $\tau_{op}$  must be sufficiently short compared to the current-quench time.

Tritium decay and Compton scattering provide energetic electrons at a rate  $\dot{n}_e$ , so the number of energetic electrons obeys the equation  $dn_e/dt = n_e/\tau_{ef} + \dot{n}_e$ , where  $\tau_{ef}$

is the time required for an e-fold in the avalanche process. That is, the time for  $\delta I$  to equal  $I_{10}/\ln(10) \approx 0.4$  MA, which is  $\tau_{ef} \sim 4$  ms when a plasma current of 15 MA is quenched in 150 ms. Assuming a constant  $\dot{n}_e$ , the solution is  $n_e(t) = \dot{n}_e\tau_{ef}(\exp(t/\tau_{ef}) - 1)$ . After a large number of e-folds,  $t \gg \tau_{ef}$ , this formula has the same form as for the exponentiation of  $n_s$  seed electrons,  $n_e(t) = n_s \exp(t/\tau_{ef})$ , so the effective number of seed electrons is

$$n_s = \dot{n}_e\tau_{ef}. \quad (46)$$

**3.4.1. Seed from tritium decay.** Tritium decays with a half-life of 12.32 years emitting an electron with a maximum energy of 18.6 keV. Assuming  $\tau_{ef} = 4$  ms and the number density of tritium nuclei is half the electron number density before the thermal quench  $n_0$ , the effective number density of seed electrons is  $n_s \approx 3 \times 10^{-12}n_0$  or  $\ell_{seed} \approx 11.5$ . A 15 MA ITER plasma could produce  $\approx 8$  MA of relativistic current starting with the tritium seed. It should be noted that the seed from tritium decay is not exponentially sensitive to plasma parameters. The uncertainty in  $\ell_{seed}$  is small, approximately 5%, primarily due to the uncertainty in  $\tau_{ef}$ .

Unfortunately, even the absence of relativistic electrons following thermal quenches in pre-nuclear phase experiments is not a proof that relativistic electrons will be unimportant during the nuclear phase.

**3.4.2. Seed from Compton scattering.** The flux of gamma rays  $\Gamma_\gamma$  in ITER is estimated to be of order  $10^{18}$  m<sup>-2</sup>s<sup>-1</sup> during strong DT power production but quickly drops to of order  $10^{15}$  m<sup>-2</sup>s<sup>-1</sup> once nuclear reactions are terminated [7]. The critical energy for runaway is proportional to the background electron density while the Compton scattering cross section is inversely proportional to the energy reached by a cold electron as a result of the scattering. Consequently the product of the background density times the Compton scattering cross section evaluated at the critical energy for runaway  $\sigma_{cp}$  is essentially independent of density with  $n_0\sigma_{cp} \approx (0.4 \times 10^{-28} \text{ m}^2)n_0$ , where  $n_0$  is the pre-thermal-quench plasma density [7]. The effective number of Compton scattering seed electrons is then  $n_s \approx n_0\sigma_{cp}\Gamma_\gamma\tau_{ef}$ . Using the gamma ray flux  $\Gamma_\gamma = 10^{15}$  m<sup>-2</sup>s<sup>-1</sup>, the effective density of seed electrons is  $n_s \approx 1.6 \times 10^{-16}n_0$ , which would require an amplification of approximately  $10^{12}$  to transfer the current. That is, a 15 MA initial current would result in a 4 MA current in relativistic electrons. The use of the flux  $\Gamma_\gamma = 10^{18}$  m<sup>-2</sup>s<sup>-1</sup> would result in a current in relativistic electrons of 7 MA.

### 3.5. Required warning time

Injecting gas-propelled pellets or gas into the ITER plasma requires at least 10 ms. Let  $f_d$  be the time delay for the arrival of pellets or gas, divided by the termination time of the ITER current. The relativistic electron current at the arrival time of the pellet or gas is  $I_{rel} = I_{p0}10^{-\ell_d}$ , where  $\ell_d = \ell_{req} - \ell_{seed} + f_d\frac{I_{p0}}{I_{10}}$ . The relativistic electron current is greater than 10% of the initial plasma current when



$$\ell_{\text{seed}} \lesssim (\ell_{\text{req}} - 1) + f_d \frac{I_{p0}}{I_{10}}. \quad (47)$$

Since  $\ell_{\text{req}} - 1 \approx 2.7$ , when the current is terminated in 50 ms,  $f_d \approx 0.2$  and the measure of the strength of the seed electrons must satisfy  $\ell_{\text{seed}} \gtrsim 6.2$  to ensure a relativistic current of at least 10% of the pre-disruption plasma current will not be driven.

If the assured warning time for thermal quenches is not adequate, much faster mitigation schemes must be investigated such as the passive system discussed in appendix D.

## 4. Discussion

In a single pulse, the plasma current in ITER goes from zero to its maximum and back to zero. What is the acceptable probability that during a single pulse relativistic electrons will cause severe machine damage? If severe machine damage implies a shutdown for months during the nuclear phase of ITER, then such events being separated by less than a year would make achievement of the ITER mission improbable. The probability of severe damage must be less than approximately one in thousand.

The probability of severe damage is the product of two probabilities. (1) The probability of an event that could lead to severe damage arising during ITER operations. (2) The probability that if the likelihood of such an event were too great that action could not be taken to avoid the damage.

The potential for severe damage is clearly present when ITER is operated at 15 MA. The question is what physical effects could make the realization of that potential sufficiently unlikely—effects that could arise either naturally or be actively imposed.

### 4.1. Mitigating effects

Two types of physical effects can mitigate the danger from relativistic electrons: (1) an increase in the density of background electrons and (2) a breaking of the magnetic surfaces. To avoid the formation of an unacceptably strong relativistic-electron current, mitigation must occur within a sufficiently short time after the initiation of a thermal quench, section 3.5. The sum of the warning time and the time required to take action must be sufficiently short.

#### 4.1.1. An increase in the density of background electrons.

- (i) *Ensure  $V_{\text{ch}} > V_{\ell}$ .* The Connor-Hastie voltage is proportional to the background electron density  $V_{\text{ch}} \propto n_b$ , so in principle the density can always be increased sufficiently to ensure that electron runaway is impossible,  $V_{\text{ch}} > V_{\ell}$ . The minimum loop voltage  $V_{\ell}$  consistent with a termination of the plasma current in 150 ms is about 500 V, which requires the density be raised several hundred times from standard value in operations. In table 5 of [4], the required density to suppress avalanche growth was given as  $4.2 \times 10^{22} \text{ m}^{-3}$ . Not only is such a large increase in the density difficult to achieve, but also it may be too small

by an order of magnitude if skin currents arise. To prevent runaway, the density averaged along every field line must be sufficiently great compared the time derivative of the poloidal magnetic flux  $\psi_p$  at fixed enclosed toroidal magnetic flux.

- (ii) *Rapidly cooling energetic electrons.* When the slowing down time for energetic particles is sufficiently short, the largest potential seed of runaway electrons, which is the high-energy tail of the hot Maxwellian, is eliminated, even when  $V_{\ell} \gg V_{\text{ch}}$ . What is required is that the slowing down time be sufficiently short compared to  $\tau_a$  and  $\tau_{\text{op}}$ . The time required for  $V_{\ell}$  to exceed  $V_{\text{ch}}$  after the start of the thermal quench is  $\tau_a$ , and the time magnetic surfaces remain broken is  $\tau_{\text{op}}$ . This strategy may well be adequate in the non-nuclear phase of ITER but would fail in nuclear phase to eliminate the seed from tritium decay unless  $\tau_a$  or  $\tau_{\text{op}}$  were comparable the the current quench time.

Runaway from tritium decay is prevented when the kinetic energy for runaway  $K_r \approx (V_{\text{ch}}/V_{\ell})m_e c^2$  exceeds the maximum energy of a beta-decay electron, 18.6 keV. Not only is the required density very large, but it is also uncertain because of the possibility of skin currents.

**4.1.2. A breaking of the confining magnetic surfaces.** A rapid breaking of magnetic surfaces is a common feature of thermal quenches whether naturally arising or as a result of the injection of material into a tokamak plasmas. When a region of stochastic magnetic field lines extends all the way to the plasma edge, passing electrons are lost too rapidly to the wall to runaway and the only energetic electrons that can remain confined are those trapped by the poloidal variation of the equilibrium magnetic field. Energetic trapped electrons are lost on a collisional time scale by detrapping and more importantly from slowing down. To be important as a seed, at least some confining magnetic surfaces must re-form before the energetic trapped particles slow down.

When all confining magnetic surfaces are broken during the thermal quench, then either the slowing down will naturally be sufficiently rapid to prevent trapped electrons from forming an important seed or material could possibly be injected to make this true.

When only a fraction of the magnetic surfaces are broken, electrons can runaway in the regions bounded by magnetic surfaces, and skin currents will naturally arise near the boundaries of these regions.

It is natural for magnetic surfaces to re-form after a thermal quench. The free energy to drive instabilities from the gradients in the plasma pressure and the parallel current are reduced during a thermal quench. The time scale of a thermal quench is so short compared to the resistive time scale of the surrounding walls that the normal magnetic field to the wall would remain unchanged from its pre-quench axisymmetric form. That is, unless subtle engineering is undertaken to use the currents induced in the walls to produce a sudden change in non-axisymmetric magnetic field normal to the wall, appendix D.

Though far from certain, it may be true that all magnetic surfaces are broken during thermal quenches and that the

surfaces remain open for a sufficiently long time that the trapped electrons do not form a seed. Even if this is true, the situation is far more difficult during the nuclear phase of ITER because of the beta-decay electrons from the tritium. The strength of the tritium decay seed is accurately given by basic physics, section 3.4.1. The magnitude is sufficiently large that if the poloidal flux change required for an e-fold in the number of electrons is correct, then unless the magnetic surfaces remain open until more than half of the poloidal flux is dissipated, a large relativistic electron current will arise. In other words, an unacceptable runaway current arises unless all confining magnetic surfaces remain broken for more than half of the current quench time.

#### 4.2. Implications

The major uncertainties in the physics of the current transfer are the value of  $\gamma_{\text{ef}}$ , equation (20), and of the strength of the electron seed  $\ell_{\text{seed}}$ , from the hot Maxwellian. A major uncertainty in the plasma state during and after the thermal quench is the spatial and temporal extent of magnetic surface breaking. The interaction of these uncertainties on the danger to ITER from relativistic electrons could be efficiently studied using the mean-field evolution equations that are derived in appendix A and discussed in section 2.3. The plasma states that can credibly arise can be studied using the mean-field evolution equations to interpret experimental data on the current spike, internal inductance, and electron temperature. The presence or absence within observational limits of relativistic electrons could provide important data on the presence or absence of confining magnetic surfaces.

It is difficult to spread injected impurities across magnetic surfaces on the time scale of the thermal quench, even Bohm diffusion  $D_B = T/eB$ , is too slow. The rapid spreading of impurities may be evidence of fast magnetic reconnection in which segments of the field lines that formed the original magnetic surfaces are spread across the plasma.

Possibly the greatest threat to the ITER mission from relativistic electrons arises from the seed electrons from tritium decay. The magnitude of the seed is essentially certain; the major uncertainties are  $\gamma_{\text{ef}}$  and the spatial and temporal extent of magnetic surface breaking. Studies using the mean-field evolution equations would greatly clarify issues such as how long the magnetic surfaces would have to remain broken to avoid an unacceptable relativistic current.

Since even one plasma pulse in a thousand ending in major damage would greatly impact the ITER mission, studies of all credible plasma conditions are required. Many cases must be investigated, so the computational effort on each case must be limited—at least until the most important cases are identified. The mean-field evolution equations, section 2.3, seem ideally suited to such studies.

In the absence of a credible strategy of preventing electron runaway following a thermal quench, ITER must be operated in as conservative manner as necessary to avoid thermal quenches. To obtain interesting plasma parameters while operating with the required conservatism may well require

a predictive code to steer the plasma. This is especially true if the required time to shut down the plasma current without disruption is the comparable to its  $L/R$  decay time,  $\sim 1000$  s.

#### Acknowledgment

This material is based upon work supported by the U.S. Department of Energy, Office of Science, Office of Fusion Energy Sciences under Award No. DE-FG02-03ER54696 and DE-SC0016347. The author would like to thank Eric Nardon and Chang Liu for helpful discussions. The two reviewers heroically proofread an earlier version and pointed out a number corrections that needed to be made.

#### Appendix A. Derivation of mean-field equation

The derivation of the evolution equation for the poloidal flux, which follows directly from Maxwell's equations, was given in [1]. Here the simpler mean-field equation for the evolution of the poloidal flux is derived.

##### A.1. Implications of Maxwell's equations

In toroidal geometry, the vector potential  $\vec{A}$  and the magnetic field  $\vec{B}$  can always be written [36] as

$$\vec{A} = \psi_t \vec{\nabla} \frac{\theta}{2\pi} - \tilde{\psi}_p \vec{\nabla} \frac{\varphi}{2\pi}; \quad (\text{A.1})$$

$$\vec{B} = \vec{\nabla} \psi_t \times \vec{\nabla} \frac{\theta}{2\pi} + \vec{\nabla} \frac{\varphi}{2\pi} \times \vec{\nabla} \tilde{\psi}_p, \quad (\text{A.2})$$

where  $\theta$  is any poloidal and  $\varphi$  is any toroidal angle. The toroidal  $\psi_t$  and the poloidal flux  $\tilde{\psi}_p$  are defined in figure 2. Actually any vector  $\vec{A}$  can be represented in the form of equation (A.1) when a term  $\vec{\nabla} g$  is added to the right hand side.

Wherever the toroidal component of the magnetic field is non-zero,  $\vec{B} \cdot \vec{\nabla} \varphi \neq 0$ ,  $(\psi_t, \theta, \varphi)$  can be used as coordinates. The position vector  $\vec{x}(\psi_t, \theta, \varphi)$  gives the location of coordinate points in space, figure 2. The Jacobian of  $(\psi_t, \theta, \varphi)$  canonical coordinates is

$$\mathcal{J} \equiv \frac{1}{(\vec{\nabla} \psi_t \times \vec{\nabla} \theta) \cdot \vec{\nabla} \varphi} = \frac{1}{2\pi \vec{B} \cdot \vec{\nabla} \varphi}. \quad (\text{A.3})$$

These coordinates are called canonical for  $\tilde{\psi}_p(\psi_t, \theta, \varphi)$  is the Hamiltonian for the magnetic field lines;  $d\psi_t/d\varphi = -\partial\tilde{\psi}_p/\partial\theta$  and  $d\theta/d\varphi = \partial\tilde{\psi}_p/\partial\psi_t$ .

When the magnetic field is time dependent, both the poloidal flux and the position vector can depend on time,  $\tilde{\psi}_p(\psi_t, \theta, \varphi, t)$  and  $\vec{x}(\psi_t, \theta, \varphi, t)$ . Faraday's law can be written in the  $(\psi_t, \theta, \varphi)$  canonical coordinates as

$$\vec{E} + \vec{u}_c \times \vec{B} = \left( \frac{\partial \tilde{\psi}_p}{\partial t} \right)_c \vec{\nabla} \frac{\varphi}{2\pi} - \vec{\nabla} \Phi_c, \quad (\text{A.4})$$

where the subscript  $c$  implies the canonical  $(\psi_t, \theta, \varphi)$  coordinates are held constant so  $\vec{u}_c \equiv \partial \vec{x}(\psi_t, \theta, \varphi, t)/\partial t$  is the velocity of the canonical coordinates through space. Equation (A.4)

has a plausible form; the derivation [1] is based on the expression  $(\partial \vec{A}/\partial t)_{\vec{x}}$  in canonical coordinates, which is given in the appendix to [36].

### A.2. Mean-field evolution of the poloidal flux

In mean-field theory, the parallel component of Ohm's law is

$$\vec{E} \cdot \vec{B} = \eta \vec{j} \cdot \vec{B} - \vec{\nabla} \cdot \left( \lambda \vec{\nabla} \frac{j_{\parallel}}{B} \right). \quad (\text{A.5})$$

The first term  $\eta \vec{j} \cdot \vec{B}$ , where  $\eta$  is the plasma resistivity, is well known. The second term, which involves second derivatives of  $\vec{j} \cdot \vec{B}/B^2$ , is an essentially unique form that transports magnetic helicity without its creation or destruction [23] and is the characteristic term of a mean-field Ohm's law. This term gives the relaxation of the current profile due to magnetic field line breaking by unresolved magnetic perturbations. The coefficient that determines the rate of transport,  $\lambda$ , must be greater than or equal to zero to avoid the relaxation process increasing the magnetic energy,  $\int j_{\parallel} E_{\parallel} d^3x = \int \lambda \{ \vec{\nabla} (j_{\parallel}/B) \}^2 d^3x$ .

The effect of broken magnetic surfaces is incorporated in mean-field theory by the coefficient  $\lambda$  rather than in the poloidal flux  $\psi_p$  being a function of all three spatial coordinates. That is, the poloidal magnetic flux is taken to be

$$\psi_p(\psi_t, t) \equiv \oint \tilde{\psi}_p(\psi_t, \theta, \varphi) \frac{d\theta}{2\pi} \frac{d\varphi}{2\pi}, \quad (\text{A.6})$$

which gives perfect magnetic surfaces. Within mean field theory only the mean poloidal flux  $\psi_p(\psi_t, t)$  appears. Equation (A.4) and the expression for the Jacobian, equation (A.3) then imply

$$\frac{\partial \psi_p(\psi_t, t)}{\partial t} = \frac{\partial}{\partial \psi_t} \int^{\psi_t} \vec{E} \cdot \vec{B} d^3x. \quad (\text{A.7})$$

The flux evolution equation is particularly easy to derive where the plasma pressure gradient is zero, then the current density  $\vec{j} = (j_{\parallel}/B)\vec{B}$  being divergence free implies  $\vec{B} \cdot \vec{\nabla} (j_{\parallel}/B) = 0$ . Otherwise, magnetic field line averages must be defined, as in [36], to remove the Pfirsch–Schlüter current, which is the part of  $j_{\parallel}/B$  that varies along a magnetic field line. Assuming  $j_{\parallel}/B$  is constant on  $\psi_t$  surfaces,

$$I(\psi_t, t) \equiv \int^{\psi_t} \oint (\vec{j} \cdot \vec{\nabla} \varphi) \mathcal{J} d\psi_t d\theta \quad (\text{A.8})$$

$$\begin{aligned} &= \int^{\psi_t} \frac{j_{\parallel}}{B} \oint (\vec{B} \cdot \vec{\nabla} \varphi) \mathcal{J} d\psi_t d\theta \\ &= \int^{\psi_t} \frac{j_{\parallel}}{B} d\psi_t, \text{ so} \end{aligned} \quad (\text{A.9})$$

$$\frac{j_{\parallel}}{B} = \frac{\partial I(\psi_t, t)}{\partial \psi_t}. \quad (\text{A.10})$$

The resistance is defined as

$$\mathcal{R}_{\psi}(\psi_t, t) \equiv \oint \frac{2\pi B^2}{\vec{B} \cdot \vec{\nabla} \varphi} \eta \frac{d\theta d\varphi}{(2\pi)^2} \text{ so} \quad (\text{A.11})$$

$$\int \eta \vec{j} \cdot \vec{B} d^3x = \int \mathcal{R}_{\psi} \frac{\partial I}{\partial \psi_t} d\psi_t. \quad (\text{A.12})$$

$\mathcal{R}_{\psi}/\psi_t$  has units of Ohms.

The characteristic mean-field term

$$\begin{aligned} \int \vec{\nabla} \cdot \left( \lambda \vec{\nabla} \frac{j_{\parallel}}{B} \right) d^3x &= \oint \lambda \left( \vec{\nabla} \frac{j_{\parallel}}{B} \right) \cdot \vec{\nabla} \psi_t \mathcal{J} d\theta d\varphi \\ &= \psi_t \Lambda_m \frac{\partial^2 I}{\partial \psi_t^2}, \text{ where} \end{aligned} \quad (\text{A.13})$$

$$\Lambda_m(\psi_t, t) \equiv \frac{\oint \lambda (\vec{\nabla} \psi_t)^2 \mathcal{J} d\theta d\varphi}{\psi_t}. \quad (\text{A.14})$$

The factor of  $\psi_t$  that appears in the denominator of equation (A.14) is required for the analyticity of the poloidal flux transport as  $\psi_t \rightarrow 0$ .

The evolution equation has the same form as in the exact expression given in [1],

$$\frac{\partial \psi_p}{\partial t} = V_{\ell} - \frac{\partial \mathcal{F}_{\parallel}}{\partial \psi_t} \text{ with the definitions} \quad (\text{A.15})$$

$$V_{\ell} \equiv \mathcal{R}_{\psi} \frac{\partial I}{\partial \psi_t} \text{ and} \quad (\text{A.16})$$

$$\mathcal{F}_{\parallel} \equiv \psi_t \Lambda \frac{\partial^2 I}{\partial \psi_t^2}, \quad (\text{A.17})$$

where  $\mathcal{F}_{\parallel}$  is the flux of poloidal magnetic flux and, therefore, magnetic helicity along the stochastic magnetic field lines in the exact theory of [1]. These three equations are equivalent to equation (3).

The mean field equations are an average over surfaces that contain a fixed toroidal magnetic flux  $\psi_t$ . When the poloidal flux, which has the general form  $\tilde{\psi}_p(\psi_t, \theta, \varphi, t)$ , is not constant on these  $\psi_t$  surfaces,  $j_{\parallel}/B$  can vary along the magnetic field lines and drive Alfvén waves that transport magnetic helicity along the field lines, which means  $\mathcal{F}_{\parallel} \neq 0$ . The constraint  $\vec{\nabla} \cdot \vec{j} = 0$ , which follows from the smallness of the Debye length [36], implies there is a Lorentz force  $\vec{j} \times \vec{B}$ , wherever  $\vec{B} \cdot \vec{\nabla} (j_{\parallel}/B) \neq 0$ . When plasma inertia balances the Lorentz force, Alfvén waves relax the variation in  $j_{\parallel}/B$  along the magnetic field lines [1, 18], which implies a non-zero flux of helicity  $\mathcal{F}_{\parallel}$  along  $\vec{B}$ . This physics effect is represented by equation (A.17).

### A.3. Generality of Ohm's law

The Ohm's law given in equation (A.5) assumes the density of parallel current carried by relativistic electrons,  $j_{\text{rel}}$  is small compared to that carried by near-thermal electrons,  $j_{\parallel} - j_{\text{rel}}$ . This assumption is appropriate for understanding whether a large fraction of the plasma current is transferred from near-thermal to relativistic electrons, which is the focus of this paper. When the current density of relativistic electrons approaches the full current density, the term  $\eta j_{\parallel}$  in the parallel electric field is replaced by  $\eta(j_{\parallel} - j_{\text{rel}})$ , or

$$\mathcal{R}_\psi \frac{dI}{d\psi_t} \rightarrow \mathcal{R}_\psi \left( \frac{dI}{d\psi_t} - \frac{dI_{\text{rel}}}{d\psi_t} \right) \quad (\text{A.18})$$

in equation (3), where  $I_{\text{rel}}(\psi_t, t)$  is the current in relativistic electrons. The magnitude of the relativistic electron current is  $|j_{\text{rel}}(t)| \approx ec n_e(t)$ , where the number of energetic electrons  $n_e(t)$  is found by solving a kinetic equation. As  $j_{\text{rel}} \rightarrow j_{\parallel}$  the electric field drops to the level at which  $dn_e/dt \rightarrow 0$ , which in heuristic theory is the Connor-Hastie electric field  $E_{\text{ch}}$ . When the temperature has dropped sufficiently to remove the poloidal flux in ITER,  $\sim 75 \text{ V} \cdot \text{s}$ , on a shorter time scale than the drift time into the walls,  $\sim 150 \text{ ms}$ , the quantity  $\eta j_{\parallel}$  must be several hundred times larger than the Connor-Hastie electric field. Consequently, the parallel electric field is very large compared to the Connor-Hastie field when  $|j_{\parallel} - j_{\text{rel}}|/|j_{\parallel}| \gg 10^{-2}$ , so the equation  $dn_e/dt = (n_e/\psi_{\text{ef}})(\partial\psi_p/\partial t)$  remains valid.

Many papers have been written justifying the form of the mean-field equation for the parallel electric field, equation (A.5); this literature can be accessed by checking the references to [23], the paper in which the concept was introduced.

#### A.4. Magnetic energy dissipation

The rate at which the energy in the poloidal magnetic field is dissipated is  $dW_p/dt = -\int j_{\parallel} E_{\parallel} d^3x$ . In a mean-field model, this implies

$$\frac{dW_p}{dt} = - \int \frac{\partial I}{\partial \psi_t} \frac{\partial \psi_p}{\partial t} d\psi_t \quad (\text{A.19})$$

$$= - \int \mathcal{R}_\psi \left( \frac{\partial I}{\partial \psi_t} \right)^2 d\psi_t - \int \psi_t \Lambda_m \left( \frac{\partial^2 I}{\partial \psi_t^2} \right)^2 d\psi_t. \quad (\text{A.20})$$

When  $\mathcal{R}_\psi = 0$ , the magnetic field energy drops at fixed helicity content, equation (A.21), until  $\partial^2 I / \partial \psi_t^2 = 0$ , which is equivalent to a spatially constant  $j_{\parallel}/B$ .

#### A.5. Magnetic helicity evolution

The magnetic helicity content of a region defined by two  $\psi_t$  surfaces in arbitrary canonical coordinates is

$$K_c(t) \equiv -2 \int \psi_p d\psi_t, \text{ so} \quad (\text{A.21})$$

$$\frac{dK_c}{dt} = -2 \int V_\ell d\psi_t + 2\mathcal{F}_{\parallel} \Big|_{\text{bnd}}. \quad (\text{A.22})$$

The helicity content flowing through the boundary is  $\mathcal{F}_{\parallel} \Big|_{\text{bnd}}$  and is zero when the boundary is a perfect conductor.

The relation between the helicity content and the usual magnetic helicity of Woltjer [37] is  $\int \vec{A} \cdot \vec{B} d^3x = K_c + \psi_p \psi_t \Big|_{\text{bnd}}$ , where  $\Big|_{\text{bnd}}$  implies evaluation on the boundary. Using Ohm's law, the dissipation of  $K_c$  within the plasma volume obeys

$$\frac{dK_c}{dt} = -2\bar{\mathcal{R}}_\psi I_p, \text{ where} \quad (\text{A.23})$$

$$\bar{\mathcal{R}}_\psi \equiv \frac{\int \mathcal{R}_\psi \frac{\partial I}{\partial \psi_t} d\psi_t}{I_p}, \quad (\text{A.24})$$

where  $I_p \equiv I(\Psi_t, t)$  is the net plasma current. The resistance  $\bar{\mathcal{R}}_\psi$  is given by a  $j_{\parallel}/B$  weighted volumetric average of the resistivity. Note that  $\bar{\mathcal{R}}_\psi/\Psi_t$  has units of Ohms, where  $\Psi_t$  is the total toroidal flux in the plasma. When there is a surface current, the resistivity  $\eta$  on that surface is heavily weighted but the resistance is not singular.

The evolution of the magnetic helicity is always on a global resistive time scale. The current profile can be flattened on an Alfvénic time scale, but when the resistive time scale, which is determined by  $\bar{\mathcal{R}}_\psi$ , is sufficiently long compared to the toroidal Alfvén transit time the flattening must occur at fixed magnetic helicity.

## Appendix B. Axisymmetric equilibrium equations

### B.1. Derivation of equilibrium equations

The dependence of axisymmetric force-free equilibria on the current profile is given in this appendix and derived in [1].

Equation (237) in [36] can be used to write the rotational transform  $\iota(\psi_t) = 1/q(\psi_t)$  as

$$\iota(\psi_t) = \frac{L(\psi_t)}{2} \frac{I(\psi_t)}{\psi_t} \text{ where} \quad (\text{B.1})$$

$$L(\psi_t) = \frac{2\kappa(\psi_t)}{1 + \kappa^2} \mu_0 R_0. \quad (\text{B.2})$$

The analyticity of the position vector  $\vec{x}(\psi_t, \theta, \varphi)$  implies geometric factor  $\kappa(\psi_t)$  in the inductance  $L(\psi_t)$  becomes the elongation of the surfaces near the magnetic axis,  $\kappa_0$ , which means as  $\psi_t \rightarrow 0$ .

$\Psi_t$  is the toroidal magnetic flux enclosed by the plasma. The poloidal flux, which obeys [36] the exact equation  $d\psi_p/d\psi_t = \iota(\psi_t)$ , the helicity content  $K_c$  of equation (A.21), the energy in the poloidal magnetic field, and the internal inductance are

$$\psi_p(\psi_t) = \int_{\Psi_t}^{\psi_t} \frac{LI}{2\psi_t} d\psi_t; \quad (\text{B.3})$$

$$K_c = -2 \int_0^{\Psi_t} \psi_p(\psi_t) d\psi_t; \quad (\text{B.4})$$

$$W_p = \frac{1}{4} \int_0^{\Psi_t} \frac{LI^2}{\psi_t} d\psi_t; \quad (\text{B.5})$$

$$\ell_i \equiv \frac{W_p}{\frac{1}{4}\mu_0 R_0 I_p^2}. \quad (\text{B.6})$$

The poloidal flux  $\psi_p(\psi_t)$  as defined in equation (B.3) is actually the poloidal flux minus its edge value  $\psi_{\text{pe}}(t)$ . The surface loop voltage is  $d\psi_{\text{pe}}/dt$ .

Given a current profile  $I(\psi_t)$ , these equations can be easily integrated when the surface-shaping factor  $\kappa$  in the inductance is assumed fixed.  $L(\psi_t)$  is then a spatial constant,



$$L_0 \equiv \frac{2\kappa_0}{1 + \kappa_0^2} \mu_0 R_0. \quad (\text{B.7})$$

When the constancy of  $\kappa$  is assumed, let

$$\ell_p \equiv \frac{1}{I_p^2} \int_0^{\Psi_t} \frac{I^2(\psi_t)}{\psi_t} d\psi_t, \text{ then} \quad (\text{B.8})$$

$$\ell_i = \frac{2\kappa_0}{1 + \kappa_0^2} \ell_p. \quad (\text{B.9})$$

## B.2. Current profile examples

Three current profiles are used in this paper: the flattop, the parabolic, and the flat.

**B.2.1. Flattop current profile.** Assume  $I(\psi_t) = I_p \psi_t / \psi_0$  for  $\psi_t < \psi_0$  and  $I(\psi_t) = I_p$  for  $\Psi_t > \psi_t > \psi_0$ . Then the poloidal flux enclosed by the magnetic axis is  $\Psi_p = -(L_0/2)(1 + \ln(\Psi_t/\psi_0))$ , and  $\ell_p = \ln(\Psi_t/\psi_0) + 1/2$ . The flux inductance,  $\mathcal{L} \equiv |\Psi_p/I_p|$ , is

$$\mathcal{L} = L_0 \frac{1 + 2\ell_p}{4}. \quad (\text{B.10})$$

**B.2.2. Parabolic current profile.** For a parabolic current profile, the current density has a parabolic dependence on the minor radius; more precisely the current density is proportional to  $dI/d\psi_t = 2(I_p/\Psi_t)(1 - \psi_t/\Psi_t)$ . The current itself is

$$I(\psi_t) = I_p \left( 2 - \frac{\psi_t}{\Psi_t} \right) \frac{\psi_t}{\Psi_t} \quad (\text{B.11})$$

$$\psi_p(\psi_t) = -L_0 I_p \left( \frac{3}{4} - \frac{\psi_t}{\Psi_t} + \frac{1}{4} \left( \frac{\psi_t}{\Psi_t} \right)^2 \right) \quad (\text{B.12})$$

$$K_c = \frac{2}{3} L_0 I_p \Psi_t \quad (\text{B.13})$$

$$\ell_p = \frac{11}{12}. \quad (\text{B.14})$$

**B.2.3. Flat current profile.** For a flat current profile, the current density is a spatial constant, or  $dI/d\psi_t = I_p/\Psi_t$ :

$$I(\psi_t) = I_p \frac{\psi_t}{\Psi_t} \quad (\text{B.15})$$

$$\psi_p(\psi_t) = -\frac{L_0 I_p}{2} \left( 1 - \frac{\psi_t}{\Psi_t} \right) \quad (\text{B.16})$$

$$K_c = \frac{1}{2} L_0 I_p \Psi_t \quad (\text{B.17})$$

$$\ell_p = \frac{1}{2}. \quad (\text{B.18})$$

## Appendix C. Magnitude of $\Lambda_m$

The equilibrium equations can be used to obtain a characteristic value for  $\Lambda_m$  and typical changes in the poloidal field energy and the plasma current during a quasi-ideal relaxation.

When a parabolic profile relaxes to a flat profile conserving helicity  $K_c$ , the ratio of the final to the initial current is  $I_{pf} = (4/3)I_{pi}$ , where the  $i$  and  $f$  subscripts denote the initial and final states. A quasi-ideal relaxation gives a larger spike than is observed in experiments. The resistivity becomes sufficiently great during a thermal quench that some helicity dissipation is expected, an amount that does not appear to be inconsistent with observations. As noted in the discussion of equation (7), without resistive relaxation a quasi-ideal relaxation can cause an increase in the plasma current only when it extends to the plasma edge. A large reduction in plasma elongation  $\kappa$  during the thermal quench could reduce the observed current spike. The relevance of this alternative explanation could be determined from a study of experimental results using the simulation methods discussed in section 2.

The ratio of the final to the initial poloidal field energy is  $W_{pf}/W_{pi} = (\ell_{pf}/\ell_{pi})(I_{pf}/I_{pi})^2 = 32/33$ . The fractional reduction in poloidal field energy is very small ( $W_{pi} - W_{pf})/W_{pi} = 1/33$ .

The poloidal field energy is dissipated during a quasi-ideal relaxation;

$$\frac{dW_p}{dt} = - \int \psi_t \Lambda_m \left( \frac{\partial^2 I}{\partial \psi_t^2} \right)^2 d\psi_t, \text{ so} \quad (\text{C.1})$$

$$= -2 \frac{\Lambda_m I_p^2}{\Psi_t^2} \quad (\text{C.2})$$

is the initial rate for the parabolic profile. The characteristic time scale for the relaxation for a parabolic profile is

$$\tau_{\text{relax}} \equiv \frac{W_{pi} - W_{pf}}{W_{pi}} \frac{W_{pi}}{dW_p/dt} \quad (\text{C.3})$$

$$= \frac{1}{288} \frac{L_0}{\Lambda_m} \Psi_t^2. \quad (\text{C.4})$$

The relaxation of the  $j_{\parallel}/B$  profile takes place through a shear Alfvén wave, which implies the relaxation time is given by  $\tau_{\text{relax}} = N_t 2\pi R_0 / V_A$ , where  $N_t$  is the number of toroidal transits required for a shear Alfvén wave to cover the stochastic region by propagating along the field lines at the speed  $V_A$ . Therefore,

$$\Lambda_m = \frac{1}{144} \frac{2\kappa_0}{1 + \kappa_0^2} \frac{\mu_0}{4\pi} \frac{V_A \Psi_t^2}{N_t}. \quad (\text{C.5})$$

Judging from the time scale of the current spike,  $N_t$  is a few hundred.

An estimate of the number of toroidal transits  $N_t$  required for a magnetic field line to cover a stochastic region can be made when  $N_i$  primary islands are involved in the stochasticization. The average width the islands is  $w \sim a/N_i$ , where  $a$  is the plasma radius. The number of toroidal circuits required for a magnetic field line to circumnavigate an island is

$N_c \sim \pi R_0/(\Delta\iota w/2)$ , where  $\Delta\iota$  is the change in the rotational transform  $\iota = 1/q$  across the region that will become stochastic. The number of transits to cross the region is then  $N_t = (a/w)^2 N_c$ , which is the number of steps squared  $(a/w)^2$  that a field line requires, going randomly around the islands, to cross the plasma times the number of toroidal transits per step. The required number of toroidal transits to cross the stochastic region is

$$N_t \sim \frac{2\pi R_0}{a\Delta\iota} N_i^3. \quad (\text{C.6})$$

Even two or three primary island chains could make  $N_t$  a few hundred

The dimensionless ratio  $\mathcal{R}_\psi \Psi_t / \Lambda_m$  gives the characteristic ratio of the rate at which magnetic energy is lost by resistive dissipation relative to a quasi-ideal relaxation,

$$\frac{\mathcal{R}_\psi \Psi_t}{\Lambda_m} \approx 576 \frac{N_t}{S}, \text{ where} \quad (\text{C.7})$$

$$S = \frac{V_A}{2\pi R_0} \frac{\mu_0 a^2}{\eta} \quad (\text{C.8})$$

is the Lundquist number and  $a$  is a minor radius defined by  $\Psi_t = \pi B a^2$ .

## Appendix D. Passive mitigation

The injection of material into the plasma may not only require a warning time that is too long but also the amount of material that must be injected has a large uncertainty because of the possibility of skin currents greatly enhancing  $E_\parallel = \eta j_\parallel$ . The most reliable method of avoiding relativistic electrons may be the destruction of all magnetic surfaces in the plasma early in the thermal quench and maintaining their destruction for a time comparable to the current-quench time. This long time may be required to avoid runaway due to tritium decay during the nuclear phase of ITER operation.

One possibility [38, 39] is to use the currents induced in the wall during the thermal quench to produce a fast change in the normal magnetic field to the wall. The important change is in the distributions that break magnetic surfaces—crudely low-order Fourier coefficients of B-normal that resonate with the safety factor within the plasma. Three types of currents are induced in the walls during a thermal quench that is on a fast time scale compared to resistive time scales in the walls: (1) A current of cosinusoidal form,  $I_v$ , arises to maintain a fixed normal magnetic field on the walls, the normal field that is associated with the vertical field required for axisymmetric equilibrium. (2) A net poloidal current,  $G_w$ , arises because the toroidal flux displaced by the plasma depends on the plasma volume, which changes during a thermal quench. (3) An equal but opposite net toroidal current  $I_w$  arises in response to any change in the net plasma current  $I_p$ .

These currents track changes with a time delay set by the cross-field Alfvén speed, which is a negligible delay. It is the resistive decay of the  $I_v$  current that gives the time

scale  $\sim 150$  ms for a plasma to drift into the chamber walls in ITER if axisymmetric control is lost.

In a large aspect ratio,  $R_0/a \rightarrow \infty$ , model of a tokamak, the toroidal magnetic flux displaced by a plasma is

$$\Psi_{td} = (1 - \beta_\theta) \frac{B_\theta^2}{2\mu_0} \frac{A_p}{B_\varphi}, \quad (\text{D.1})$$

where  $\beta_\theta \equiv 2\mu_0 \bar{p}/B_\theta^2$ , the volume-averaged pressure is  $\bar{p}$ , the edge poloidal field is  $B_\theta$ , and the cross-sectional area of the plasma is  $A_p$ . If the plasma pressure is suddenly lost through radiation but the magnetic field responds ideally, the toroidal flux within the plasma, the safety factor  $q$  within the plasma, and the toroidal flux enclosed by the surrounding wall remain fixed. The toroidal flux in the plasma is held fixed by a change in the external toroidal field  $B_\varphi$  and the cross-sectional area of the plasma  $A_p$ . Since  $B_\varphi$  changes little across the plasma,  $\delta\Psi_{td} + \delta(B_\varphi A_p) = 0$ . The toroidal flux enclosed by the wall is held fixed by holding the toroidal flux in the annular region between the wall and the plasma fixed,  $\delta(B_\varphi(A_w - A_p)) = 0$ , where  $A_w$  is the cross-sectional area enclosed by the wall. That is, the change in the plasma area is  $\delta A_p = (A_w - A_p)(\delta B_\varphi/B_\varphi)$ . When the area of the annular region is small compared to that of the plasma,  $(A_w - A_p)/A_p \ll 1$ , the change in the plasma area is negligible and the change in the toroidal field in the annular region is  $\delta B_\varphi = -\delta\Psi_{td}/A_p$ . Since the safety factor and geometry of the plasma are unchanged, the change in the poloidal field is  $\delta B_\theta = (\delta B_\varphi/B_\varphi)B_\theta$ . The current induced in the wall  $G_w = 2\pi R_0 \delta B_\varphi/\mu_0$ .

It should be noted that whatever the shape of the chamber walls, there is a spatial distribution of poloidal current and of toroidal current that produces no normal magnetic field on a surface that coincides with the chamber walls. If the chamber walls were perfect conductors this is the distribution of toroidal and poloidal current that would be induced when  $I_v$  is defined as the current in the chamber walls required to maintain an unchanged axisymmetric normal magnetic field on the walls.

To enhance the destruction of magnetic surfaces on the time scale of the fast magnetic reconnection, the normal magnetic field to the chamber walls must be changed on this time scale. This means on a time scale  $\sim 1$  ms, which is much shorter than time scales for currents to resistively decay in the walls,  $\sim 150$  ms as defined by the decay of  $I_v$ . A rapid  $\sim 1$  ms change in the normal magnetic field on the walls implies the walls must prevent or have a very high resistance to currents from flowing in certain directions.

To prevent a current transfer to relativistic electrons due to the seed from tritium decay, it may be necessary to maintain magnetic surface breaking until most of the poloidal flux is dissipated by the current quench. The time of the current quench must be comparable or shorter than the time scale for the current associated with the vertical field  $I_v$  to decay. Fortunately, the decay of the plasma current induces all three types of current,  $I_v$ ,  $G_w$ , and  $I_w$ , which could be used to maintain magnetic surface breaking.

Unless the walls are designed to rapidly produce non-axisymmetric magnetic perturbations, magnetic surfaces are

expected to re-form after a thermal quench. The drive for large-scale surface breaking instabilities, pressure and current gradients, are greatly reduced by the breaking of the magnetic surfaces during the thermal quench, and unless the magnetic field normal to the chamber walls changes rapidly compared to the resistive time scale of the walls, the external boundary conditions are axisymmetric.

The ITER walls are not designed to be consistent with passive mitigation. Two types of studies are needed to assess the feasibility of passive mitigation: (1) An investigation of the magnitude and spatial distribution of magnetic fields that would be required to enhance and extend the breakup of magnetic surfaces. (2) A study of whether walls can be designed that produce long-wavelength non-axisymmetric perturbations when carrying the currents  $I_v$ ,  $G_w$ , and  $I_w$ . These studies could initially be carried out independently to establish feasibility, but must eventually be made self-consistent.

## References

- [1] Boozer A.H. 2017 *Nucl. Fusion* **57** 056018
- [2] Rosenbluth M.N. and Putvinski S.V. 1997 *Nucl. Fusion* **37** 1355
- [3] Jayakumar R., Fleischmann H.H. and Zweben S.J. 1993 *Phys. Lett. A* **172** 447
- [4] Hender T.C. *et al* 2007 Progress in the ITER physics basis chapter 3: MHD stability, operational limits and disruptions *Nucl. Fusion* **47** S128–202
- [5] Helander P., Eriksson L.-G. and Andersson F. 2002 *Plasma Phys. Control. Fusion* **44** B247
- [6] Lehnen M. 2017 *Executive Report ITER Disruption Mitigation Workshop (ITER HQ, 8–10 March 2017)* (<http://www.firefusionpower.org/#NewsSection>)
- [7] Martín-Solís J.R., Loarte A. and Lehnen M. 2017 *Nucl. Fusion* **57** 066025
- [8] de Vries P.C. *et al*, The COMPASS Team, The ASDEX Upgrade Team and JET Contributors 2016 *Nucl. Fusion* **56** 026007
- [9] Berger M.A. 1984 *Geophys. Astrophys. Fluid Dyn.* **30** 79
- [10] Aleynikov P. and Breizman B.N. 2017 *Nucl. Fusion* **57** 046009
- [11] Boozer A.H. 2016 *Phys. Plasmas* **23** 082514
- [12] Boozer A.H. and Punjabi A. 2016 *Phys. Plasmas* **23** 102513
- [13] Rutherford P.H. 1973 *Phys. Fluids* **16** 1903
- [14] Zweibel E.G. and Yamada M. 2016 *Proc. R. Soc. A* **472** 20160479
- [15] Loureiro N.F. and Uzdensky D.A. 2016 Magnetic reconnection: from the Sweet-Parker model to stochastic plasmoid chains *Plasma Phys. Control. Fusion* **58** 014021
- [16] Comisso L. and Bhattacharjee A. 2016 On the value of the reconnection rate *J. Plasma Phys.* **82** 595820601
- [17] Boozer A.H. 2013 *Phys. Plasmas* **20** 032903
- [18] Boozer A.H. 2014 *Phys. Plasmas* **21** 072907
- [19] Izzo V.A. *et al* 2011 *Nucl. Fusion* **51** 063032
- [20] Izzo V.A., Humphreys D.A. and Kornbluth M. 2012 *Plasma Phys. Control. Fusion* **54** 095002
- [21] Fil A. *et al* and JET Contributors 2015 *Phys. Plasmas* **22** 062509
- [22] Nardon E., Huijsmans G., Fil A. and Hoelzl M. 2017 *Plasma Phys. Control. Fusion* **59** 014006
- [23] Boozer A.H. 1986 *J. Plasma Phys.* **35** 133
- [24] Jardin S., Chen J., Ferraro N. and Pfefferle D. 2017 M3D-C1 simulation of a current ramp-down disruption in NSTX *Presentation at the Theory, Simulation of Disruptions Workshop at the Princeton Plasma Physics Laboratory (Princeton, NJ, USA, 19 July 2017)* (<http://tsdw.pppl.gov/Program.html>)
- [25] Breslau J., Ferraro N. and Jardin S. 2009 *Phys. Plasmas* **16** 092503
- [26] Boozer A.H. 2015 *Phys. Plasmas* **22** 032504
- [27] Mackay R.S., Meiss J.D. and Percival I.C. 1984 *Physica D* **13** 55–81
- [28] Meiss J.D. 2015 *Chaos* **25** 097602
- [29] Connor J.W. and Hastie R.J. 1975 *Nucl. Fusion* **15** 415
- [30] Solodov A.A. and Betti R. 2008 *Phys. Plasmas* **15** 042707
- [31] Smith H., Helander P., Eriksson L.-G., Anderson D., Lisak M. and Andersson F. 2006 *Phys. Plasmas* **13** 102502
- [32] Fleischmann H.H. and Zweben S.J. 1993 *Evaluation of Potential Runaway Generation in Large-Tokamak Disruptions (Report PPPL-2914)* (Princeton, NJ: Princeton University Plasma Physics Laboratory)
- [33] Karney C.F.F. and Fisch N.J. 1985 *Phys. Fluids* **28** 116
- [34] Smith H.M. and Verwichte E. 2008 *Phys. Plasmas* **15** 072502
- [35] Izzo V.A. and Parks P.B. 2017 *Phys. Plasmas* **24** 060705
- [36] Boozer A.H. 2015 *Nucl. Fusion* **55** 025001
- [37] Woltjer L. 1958 *Proc. Natl. Acad. Sci. USA* **44** 489
- [38] Boozer A.H. 2011 *Plasma Phys. Control. Fusion* **53** 084002
- [39] Smith H.M., Boozer A.H. and Helander P. 2013 *Phys. Plasmas* **20** 072505